

Where are the hidden-charm hexaquarks?

Zhe Liu^{1,2,*}, Hong-Tao An,^{1,2,†} Zhan-Wei Liu^{1,2,3,‡} and Xiang Liu^{1,2,3,§}

¹School of Physical Science and Technology, Lanzhou University, Lanzhou 730000, China

²Research Center for Hadron and CSR Physics, Lanzhou University and Institute of Modern Physics of CAS, Lanzhou 730000, China

³Lanzhou Center for Theoretical Physics, Key Laboratory of Theoretical Physics of Gansu Province, and Frontiers Science Center for Rare Isotopes, Lanzhou University, Lanzhou 730000, China



(Received 7 December 2021; accepted 18 January 2022; published 3 February 2022)

In this work, we carry out the study of hidden-charm hexaquark states with the typical configurations $qqc\bar{q}\bar{q}c$ ($q = u, d, s$). The mass spectra of hidden-charm hexaquark states are obtained within the chromomagnetic interaction model. In addition to the mass spectra analysis, we further illustrate their two-body strong decay behaviors. There exist some compact bound states which cannot decay through the strong interaction. Hopefully our results will help to search for such types of the exotic states in future experiments.

DOI: 10.1103/PhysRevD.105.034006

I. INTRODUCTION

With the improvement of the luminosity and precision in experiment, more and more charmoniumlike XYZ states and P_c states have been observed [1–11]. The present situation of hadronic states is far beyond the conventional quark model. The first doubly charm tetraquark T_{cc}^+ with the configuration $cc\bar{u}\bar{d}$ was observed by the LHCb Collaboration [12], and this newly discovered particle is explicitly an exotic state which cannot be classified into the conventional mesons.

The hexaquark states were proposed and the spectra of light-flavored hexaquarks were dynamically investigated very early after the birth of quark model. The $d^*(2380)$ resonance with $I(J^P) = 0(3^+)$ has been reported by CELSIUS/WASA and WASA-at-COSY Collaborations [13–15], and it is expected to be a dibaryon which contains 6 constituent quarks. The deuteron is also a dibaryon. Jaffe first found the H particle whose hyperfine interaction is much larger than that for two separated Λ baryons within the chromomagnetic interaction model [16], and this dibaryon $uuddss$ was also studied within other framework [17–24]. Moreover, the heavy dibaryons ($qqqqQQ$) [25–29], doubly heavy dibaryons ($qqqqQ\bar{Q}$)

[29–35], triply heavy dibaryons ($qqqQQQ$) [36–38], the other fully light dibaryons ($qqqqqq$) [39–44], and even fully heavy dibaryons ($QQQQQQ$) [45] were also proposed and discussed.

The hadronic states composed of three quarks and three antiquarks are another class of hexaquarks. The hidden-charm and hidden-bottom hexaquarks are especially focused on since they have much larger masses and thus are more easily distinguished from the ordinary mesons. With the hidden-charm tetraquark and pentaquark states observed in experiment, the discovery of hidden-charm hexaquarks would also come true in the future.

Very recently, BESIII collaboration measured the cross section of the process $e^+e^- \rightarrow \pi^+\pi^-\psi(3686)$ and further confirms the existence of three charmoniumlike states wherein $Y(4660)$ is closed to the threshold of $\Lambda_c\bar{\Lambda}_c$ systems [46]. Before this, the structure $Y(4660)$ has been observed in the process of $e^+e^- \rightarrow \gamma_{\text{ISR}}\pi^+\pi^-\psi(3686)$ in the Belle and BABAR experiments [47–49]. $Y(4660)$ was interpreted as a higher charmonium in Ref. [50] and a hexaquark state configured by the triquark-antitriquark clusters in Ref. [51]. The charmonium states can very likely be bound inside light hadronic matters, and such hadro-charmonium may explain the properties of the $Y(4660)$ peak [52]. G. Cotugno *et al.* suggested that the two observations of $Y(4660)$ and $Y(4630)$ are likely to be due to the same state constituted by four quarks in Ref. [53].

The $\Lambda_c\bar{\Lambda}_c$ structure was introduced to explain the production and decays of $Y(4260)$ in Refs. [51,54,55]. $Y(4630)$ was observed in process $e^+e^- \rightarrow \Lambda_c\bar{\Lambda}_c$ in the Belle experiments [56] and is considered as a candidate of $\Lambda_c\bar{\Lambda}_c$ bound state [57]. Especially, heavy baryon chiral perturbation theory was applied to systematically study the

*zhliu20@lzu.edu.cn

†anht14@lzu.edu.cn

‡liuzhanwei@lzu.edu.cn

§xiangliu@lzu.edu.cn

Published by the American Physical Society under the terms of the Creative Commons Attribution 4.0 International license. Further distribution of this work must maintain attribution to the author(s) and the published article's title, journal citation, and DOI. Funded by SCOAP³.

Λ_c - $\bar{\Lambda}_c$, Σ_c - $\bar{\Sigma}_c$, and Λ_b - $\bar{\Lambda}_b$ systems [58], and the results suggest that $Y(4260)$ and $Y(4360)$ could be Λ_c - $\bar{\Lambda}_c$ baryonia. The two states are also suggested to be a mixture, with mixing close to maximal, of two states of hadrocharmonium [59].

The masses of baryonia with the open and hidden charm, bottomness and strangeness are studied in the framework of dispersion relation technique in Refs. [60–62]. The heavy baryon-antibaryon molecule states are investigated within the effective field theory [63]. The hidden-charm and hidden-bottom hexaquark states were discussed within the QCD sum rules [64,65].

These work stimulate us to further study the hidden-charm hexaquark states. In this work we systematically investigate their mass spectra, stability, and two-body decay within the chromomagnetic interaction (CMI) model.

The simple chromomagnetic interaction arises from the one-gluon-exchange potential and further causes the mass splittings [66,67]. The CMI model has been successfully adopted to study the mass spectra and stability of multi-quark states [68–88]. The method can catch the basic features of hadron spectra, since the mass splittings between hadrons reflect the basic symmetries of their inner structures.

This paper is organized as follows. In Sec. II, the adopted CMI model and relevant parameters are introduced. We construct the flavor \otimes color \otimes spin wave functions for the S -wave hidden-charm hexaquark system in Sec. III, and study the mass spectrum and the two-body decays through the strong interaction in Sec. IV. A short summary follows in Sec. V.

II. THE HAMILTONIAN IN THE CMI MODEL

In the CMI model, the Hamiltonian has a simple form

$$H = \sum_i^6 m_i + H_{\text{CMI}},$$

$$H_{\text{CMI}} = -\sum_{i < j} C_{ij} \lambda_i \cdot \lambda_j \sigma_i \cdot \sigma_j, \quad (1)$$

where m_i is the effective mass of the i th constituent (anti)quark, and λ_i and σ_i are Gell-Mann and Pauli matrices, respectively. For the antiquark, $\lambda_{\bar{q}} = -\lambda_q^*$ and $\sigma_{\bar{q}} = \sigma_q^*$. The dynamical effect of spatial wavefunctions plays an important role in the study of hadron spectrum. Chromomagnetic interaction is nonrelativistic in the Schrödinger equation in Ref. [89] wherein the authors used the spatial wave functions with harmonic-oscillator expansion. The C_{ij} is effective coupling constant between the i th (anti)quark and j th (anti)quark

$$C_{ij} = \frac{\pi \langle \alpha_s(r) \delta^3(\mathbf{r}) \rangle}{6m_i m_j}, \quad (2)$$

TABLE I. The effective coupling parameters in units of MeV.

m_{nn}	m_{ns}	m_{ss}	m_{nc}	$m_{n\bar{n}}$	$m_{n\bar{s}}$	$m_{s\bar{s}}$	$m_{n\bar{c}}$	$m_{c\bar{c}}$
182.2	226.7	262.3	520.0	166.49	204.2	241.1	493.3	767.1
v_{nn}	v_{ns}	v_{ss}	v_{nc}	$v_{n\bar{n}}$	$v_{n\bar{s}}$	$v_{s\bar{s}}$	$v_{n\bar{c}}$	$v_{c\bar{c}}$
19.1	13.3	12.2	3.9	20.5	14.2	10.3	6.6	5.3

which is directly related to the spatial wave functions and the constituent quark masses. We focus on ground states in S -wave, and we simply suppose it does not change for various hexaquark systems.

Høgaasen *et al.* found out that the b quark mass in bottomonium is much lighter than the one in the heavy-light system, and introduced the color interaction (the spin-independent color Coulomb-like terms in the one-gluon-exchange interactions) in Refs. [83–85]. We also introduce a color term into our model Refs. [83,85]

$$H_C = -\sum_{i < j} A_{ij} \lambda_i \cdot \lambda_j. \quad (3)$$

The nonvanishing color interaction coefficient A_{ij} implies a change of the effective masses. We can rewrite the CMI Hamiltonian as Ref. [85]

$$H = -\frac{3}{4} \sum_{i < j} m_{ij} \lambda_i \cdot \lambda_j - \sum_{i < j} v_{ij} \lambda_i \cdot \lambda_j \sigma_i \cdot \sigma_j, \quad (4)$$

where

$$m_{ij} = \frac{1}{4} (m_i + m_j) + \frac{4}{3} A_{ij}. \quad (5)$$

To estimate the mass spectra of the hidden-charm hexaquark states, we extract the effective coupling parameters m_{ij} and v_{ij} from the conventional hadron masses [85]. In the present work, $v_{q\bar{q}}$ and $m_{q\bar{q}}$ are only determined by vector mesons ($q = n, s$ and $n = u, d$). We present the obtained effective coupling parameters in Table I.

III. THE WAVE FUNCTIONS

In order to calculate the CMI Hamiltonian, we need to exhaust all the possible spin and color wave functions of hexaquark states and combine them with the corresponding flavor wave functions. The constructed flavor-color-spin wave functions should be fully antisymmetric when exchanging identical quarks because of Pauli principle. The wave functions do not change with different sets of basis, and we use the $[(q_1 q_2)c][(\bar{q}_3 \bar{q}_4)\bar{c}]$ basis to construct the hidden-charm hexaquarks wave functions.

First, we discuss the flavor wave functions. The mass hierarchy for c, s , and ud quarks is obvious and we neglect the mixing effect among the $c\bar{c}$, $s\bar{s}$, and $n\bar{n}$ pairs. Based on

TABLE II. All possible flavor combinations for the hidden-charm hexaquark system.

System	Flavor combinations		
$q q c \bar{q} \bar{q} \bar{c}$	$n n c \bar{n} \bar{n} \bar{c}$	$s s c \bar{s} \bar{s} \bar{c}$	$n s c \bar{n} \bar{s} \bar{c}$
	$n s c \bar{n} \bar{n} \bar{c}$ ($n n c \bar{n} \bar{s} \bar{c}$)	$n n c \bar{s} \bar{s} \bar{c}$ ($s s c \bar{n} \bar{n} \bar{c}$)	$n s c \bar{s} \bar{s} \bar{c}$ ($s s c \bar{n} \bar{s} \bar{c}$)

these, we list all the possible flavor combinations for the hidden-charm hexaquark system in Table II.

In Table II, the three subsystems of the first line are pure neutral particles and C parity is “good” quantum number.

For the six subsystems of the second line, every subsystem has a charge conjugation antipartner, thus they have the same mass spectra, and we only need to discuss one of two relevant subsystems. In the first line of Table II, $n n c \bar{n} \bar{n} \bar{c}$ has isospin $I = (2, 1, 0)$ and $n s c \bar{n} \bar{s} \bar{c}$ has isospin $I = (1, 0)$. In the second line, the isospin I can be $(3/2, 1/2)$ for $n s c \bar{n} \bar{n} \bar{c}$, $(1, 0)$ for $n n c \bar{s} \bar{s} \bar{c}$, and $1/2$ for $n s c \bar{s} \bar{s} \bar{c}$.

Next, we briefly introduce the color wave functions for all hexaquark systems. They can be deduced from the following direct product:

$$\begin{aligned}
 ([3] \otimes [3] \otimes [3]) \otimes ([\bar{3}] \otimes [\bar{3}] \otimes [\bar{3}]) &= ([1_A] \oplus [8_{MA}] \oplus [8_{MS}] \oplus [10_S]) \otimes ([1_A] \oplus [8_{MA}] \oplus [8_{MS}] \oplus [\bar{10}_S]) \\
 &\rightarrow ([1_A] \otimes [1_A]) \oplus ([8_{MA}] \otimes [8_{MA}]) \oplus ([8_{MS}] \otimes [8_{MA}]) \\
 &\quad \oplus ([8_{MA}] \otimes [8_{MS}]) \oplus ([8_{MS}] \otimes [8_{MS}]) \oplus ([10_S] \otimes [\bar{10}_S]),
 \end{aligned} \tag{6}$$

where A (S) means totally symmetric (antisymmetric), and MS (MA) means that $q_1 q_2$ or $\bar{q}_3 \bar{q}_4$ is symmetric (antisymmetric). Here, the color-singlet wave functions for the hexaquarks are shown in Table III. In the notation $|[(q_1 q_2)^{\text{color1}} c]^{\text{color3}} [(\bar{q}_3 \bar{q}_4)^{\text{color2}} \bar{c}]^{\text{color4}}\rangle$, the color1, color2,

color3, and color4 stand for the color representations of $q_1 q_2$, $\bar{q}_3 \bar{q}_4$, $q_1 q_2 c$, and $\bar{q}_3 \bar{q}_4 \bar{c}$, respectively.

Lastly, the spin wave functions for the hidden-charm hexaquark states are also shown in Table III. In the notation $|[(q_1 q_2)_{\text{spin1}} c]_{\text{spin3}} [(\bar{q}_3 \bar{q}_4)_{\text{spin2}} \bar{c}]_{\text{spin4}}\rangle_{\text{spin5}}$, the spin1, spin2,

TABLE III. All possible color and spin wave functions for the hidden-charm hexaquark system.

Color wave functions

$$\begin{aligned}
 \phi_1^{\text{AA}} &= |[(q_1 q_2)^{\bar{3}} c]^1 [(\bar{q}_3 \bar{q}_4)^3 \bar{c}]^1\rangle \\
 \phi_3^{\text{MSMA}} &= |[(q_1 q_2)^6 c]^8 [(\bar{q}_3 \bar{q}_4)^3 \bar{c}]^8\rangle \\
 \phi_5^{\text{MSMS}} &= |[(q_1 q_2)^6 c]^8 [(\bar{q}_3 \bar{q}_4)^6 \bar{c}]^8\rangle
 \end{aligned}$$

Spin wave functions

Spin = 0:

$$\begin{aligned}
 \chi_1^{\text{MSMS}} &= |[(q_1 q_2)_1 c]_{\frac{1}{2}} [(\bar{q}_3 \bar{q}_4)_1 \bar{c}]_{\frac{1}{2}}\rangle_0 \\
 \chi_3^{\text{MSA}} &= |[(q_1 q_2)_1 c]_{\frac{1}{2}} [(\bar{q}_3 \bar{q}_4)_0 \bar{c}]_{\frac{1}{2}}\rangle_0 \\
 \chi_5^{\text{AA}} &= |[(q_1 q_2)_0 c]_{\frac{1}{2}} [(\bar{q}_3 \bar{q}_4)_0 \bar{c}]_{\frac{1}{2}}\rangle_0
 \end{aligned}$$

Spin = 1:

$$\begin{aligned}
 \chi_6^{\text{MSMS}} &= |[(q_1 q_2)_1 c]_{\frac{1}{2}} [(\bar{q}_3 \bar{q}_4)_1 \bar{c}]_{\frac{1}{2}}\rangle_1 \\
 \chi_8^{\text{MSS}} &= |[(q_1 q_2)_1 c]_{\frac{1}{2}} [(\bar{q}_3 \bar{q}_4)_1 \bar{c}]_{\frac{3}{2}}\rangle_1 \\
 \chi_{10}^{\text{MSA}} &= |[(q_1 q_2)_1 c]_{\frac{1}{2}} [(\bar{q}_3 \bar{q}_4)_0 \bar{c}]_{\frac{3}{2}}\rangle_1 \\
 \chi_{12}^{\text{AMS}} &= |[(q_1 q_2)_0 c]_{\frac{1}{2}} [(\bar{q}_3 \bar{q}_4)_1 \bar{c}]_{\frac{1}{2}}\rangle_1 \\
 \chi_{14}^{\text{AA}} &= |[(q_1 q_2)_0 c]_{\frac{1}{2}} [(\bar{q}_3 \bar{q}_4)_0 \bar{c}]_{\frac{1}{2}}\rangle_1
 \end{aligned}$$

Spin = 2:

$$\begin{aligned}
 \chi_{15}^{\text{SS}} &= |[(q_1 q_2)_1 c]_{\frac{3}{2}} [(\bar{q}_3 \bar{q}_4)_1 \bar{c}]_{\frac{3}{2}}\rangle_2 \\
 \chi_{17}^{\text{MSS}} &= |[(q_1 q_2)_1 c]_{\frac{1}{2}} [(\bar{q}_3 \bar{q}_4)_1 \bar{c}]_{\frac{5}{2}}\rangle_2 \\
 \chi_{19}^{\text{AS}} &= |[(q_1 q_2)_0 c]_{\frac{1}{2}} [(\bar{q}_3 \bar{q}_4)_1 \bar{c}]_{\frac{3}{2}}\rangle_2
 \end{aligned}$$

Spin = 3:

$$\chi_{20}^{\text{SS}} = |[(q_1 q_2)_1 c]_{\frac{3}{2}} [(\bar{q}_3 \bar{q}_4)_1 \bar{c}]_{\frac{3}{2}}\rangle_3$$

$$\begin{aligned}
 \phi_2^{\text{MAMA}} &= |[(q_1 q_2)^{\bar{3}} c]^8 [(\bar{q}_3 \bar{q}_4)^3 \bar{c}]^8\rangle \\
 \phi_4^{\text{MAMS}} &= |[(q_1 q_2)^{\bar{3}} c]^8 [(\bar{q}_3 \bar{q}_4)^6 \bar{c}]^8\rangle \\
 \phi_6^{\text{SS}} &= |[(q_1 q_2)^6 c]^{10} [(\bar{q}_3 \bar{q}_4)^6 \bar{c}]^{10}\rangle
 \end{aligned}$$

$$\begin{aligned}
 \chi_2^{\text{SS}} &= |[(q_1 q_2)_1 c]_{\frac{3}{2}} [(\bar{q}_3 \bar{q}_4)_1 \bar{c}]_{\frac{3}{2}}\rangle_0 \\
 \chi_4^{\text{AMS}} &= |[(q_1 q_2)_0 c]_{\frac{1}{2}} [(\bar{q}_3 \bar{q}_4)_1 \bar{c}]_{\frac{1}{2}}\rangle_0
 \end{aligned}$$

$$\begin{aligned}
 \chi_7^{\text{SS}} &= |[(q_1 q_2)_1 c]_{\frac{3}{2}} [(\bar{q}_3 \bar{q}_4)_1 \bar{c}]_{\frac{3}{2}}\rangle_1 \\
 \chi_9^{\text{SMS}} &= |[(q_1 q_2)_1 c]_{\frac{1}{2}} [(\bar{q}_3 \bar{q}_4)_1 \bar{c}]_{\frac{5}{2}}\rangle_1 \\
 \chi_{11}^{\text{SA}} &= |[(q_1 q_2)_1 c]_{\frac{3}{2}} [(\bar{q}_3 \bar{q}_4)_0 \bar{c}]_{\frac{1}{2}}\rangle_1 \\
 \chi_{13}^{\text{AS}} &= |[(q_1 q_2)_0 c]_{\frac{1}{2}} [(\bar{q}_3 \bar{q}_4)_1 \bar{c}]_{\frac{3}{2}}\rangle_1
 \end{aligned}$$

$$\begin{aligned}
 \chi_{16}^{\text{SMS}} &= |[(q_1 q_2)_1 c]_{\frac{3}{2}} [(\bar{q}_3 \bar{q}_4)_1 \bar{c}]_{\frac{1}{2}}\rangle_2 \\
 \chi_{18}^{\text{SA}} &= |[(q_1 q_2)_1 c]_{\frac{1}{2}} [(\bar{q}_3 \bar{q}_4)_0 \bar{c}]_{\frac{1}{2}}\rangle_2
 \end{aligned}$$

TABLE IV. All possible types of total wave functions and different classes of the hidden-charm hexaquark system.

All possible types of total wave functions for the hexaquark system without C parity		All possible types of total wave functions for the pure neutral hexaquark system	
$[\phi^{AA} \otimes \chi^{SS}] \delta_{12}^S \delta_{34}^A$	$[\phi^{MAMA} \otimes \chi^{SS}] \delta_{12}^A \delta_{34}^A$	$[\phi^{SS} \otimes \chi^{SS}] \delta_{12}^S \delta_{34}^A$	$[\phi^{MSMS} \otimes \chi^{SS}] \delta_{12}^S \delta_{34}^A$
$[\phi^{AA} \otimes \chi^{SA}] \delta_{12}^A \delta_{34}^S$	$[\phi^{MAMA} \otimes \chi^{SA}] \delta_{12}^A \delta_{34}^S$	$[\phi^{MSMS} \otimes \chi^{SA}] \delta_{12}^S \delta_{34}^A$	$[\phi^{MSMS} \otimes \chi^{SA}] \delta_{12}^S \delta_{34}^A$
$[\phi^{AA} \otimes \chi^{AS}] \delta_{12}^A \delta_{34}^A$	$[\phi^{MAMA} \otimes \chi^{AS}] \delta_{12}^A \delta_{34}^A$	$[\phi^{MSMS} \otimes \chi^{AS}] \delta_{12}^A \delta_{34}^A$	$[\phi^{MSMS} \otimes \chi^{AS}] \delta_{12}^A \delta_{34}^A$
$[\phi^{AA} \otimes \chi^{AA}] \delta_{12}^S \delta_{34}^S$	$[\phi^{MAMA} \otimes \chi^{AA}] \delta_{12}^A \delta_{34}^S$	$[\phi^{SS} \otimes \chi^{AA}] \delta_{12}^A \delta_{34}^S$	$[\phi^{MSMS} \otimes \chi^{AA}] \delta_{12}^A \delta_{34}^S$
$[\phi^{AA} \otimes \chi^{SMS}] \delta_{12}^A \delta_{34}^A$	$[\phi^{MAMA} \otimes \chi^{SMS}] \delta_{12}^A \delta_{34}^A$	$[\phi^{SS} \otimes \chi^{SMS}] \delta_{12}^A \delta_{34}^S$	$[\phi^{MSMS} \otimes \chi^{SMS}] \delta_{12}^A \delta_{34}^S$
$[\phi^{AA} \otimes \chi^{MSS}] \delta_{12}^A \delta_{34}^A$	$[\phi^{MAMA} \otimes \chi^{MSS}] \delta_{12}^A \delta_{34}^A$	$[\phi^{SS} \otimes \chi^{MSS}] \delta_{12}^A \delta_{34}^A$	$[\phi^{MSMS} \otimes \chi^{MSS}] \delta_{12}^A \delta_{34}^A$
$[\phi^{AA} \otimes \chi^{MSA}] \delta_{12}^A \delta_{34}^S$	$[\phi^{MAMA} \otimes \chi^{MSA}] \delta_{12}^A \delta_{34}^S$	$[\phi^{SS} \otimes \chi^{MSA}] \delta_{12}^A \delta_{34}^S$	$[\phi^{MSMS} \otimes \chi^{MSA}] \delta_{12}^A \delta_{34}^S$
$[\phi^{AA} \otimes \chi^{AMS}] \delta_{12}^A \delta_{34}^A$	$[\phi^{MAMA} \otimes \chi^{AMS}] \delta_{12}^A \delta_{34}^A$	$[\phi^{SS} \otimes \chi^{AMS}] \delta_{12}^A \delta_{34}^A$	$[\phi^{MSMS} \otimes \chi^{AMS}] \delta_{12}^A \delta_{34}^A$
$[\phi^{AA} \otimes \chi^{MSMS}] \delta_{12}^A \delta_{34}^A$	$[\phi^{MAMA} \otimes \chi^{MSMS}] \delta_{12}^A \delta_{34}^A$	$[\phi^{SS} \otimes \chi^{MSMS}] \delta_{12}^A \delta_{34}^A$	$[\phi^{MSMS} \otimes \chi^{MSMS}] \delta_{12}^A \delta_{34}^A$
All possible types of total wave functions for the pure neutral hexaquark system			
$[\phi^{SS} \otimes \chi^{SS}] \delta_{12}^S \delta_{34}^A$	$[\phi^{SS} \otimes \chi^{AA}] \delta_{12}^A \delta_{34}^A$	$[\phi^{MSMS} \otimes \chi^{SS}] \delta_{12}^S \delta_{34}^A$	$[\phi^{MSMS} \otimes \chi^{AA}] \delta_{12}^A \delta_{34}^A$
$[\phi^{AA} \otimes \chi^{SS}] \delta_{12}^A \delta_{34}^A$	$[\phi^{AA} \otimes \chi^{AA}] \delta_{12}^S \delta_{34}^A$	$[\phi^{MAMA} \otimes \chi^{SS}] \delta_{12}^S \delta_{34}^A$	$[\phi^{MAMA} \otimes \chi^{AA}] \delta_{12}^S \delta_{34}^A$
$\frac{1}{\sqrt{2}} [(\phi^{MAMS} \pm \phi^{MSMA}) \otimes \chi^{SS}] \delta_{12}^S \delta_{34}^A$	$\frac{1}{\sqrt{2}} [(\phi^{MAMS} \pm \phi^{MSMA}) \otimes \chi^{AA}] \delta_{12}^S \delta_{34}^A$	$\frac{1}{\sqrt{2}} [(\phi^{MAMS} \pm \phi^{MSMA}) \otimes \chi^{MSMS}] \delta_{12}^S \delta_{34}^A$	$\frac{1}{\sqrt{2}} [(\phi^{MAMS} \pm \phi^{MSMA}) \otimes \chi^{MSA}] \delta_{12}^S \delta_{34}^A$
$\frac{1}{\sqrt{2}} [\phi^{SS} \otimes (\chi^{SA} \pm \chi^{AS})] \delta_{12}^S \delta_{34}^A$	$\frac{1}{\sqrt{2}} [\phi^{AA} \otimes (\chi^{SA} \pm \chi^{AS})] \delta_{12}^A \delta_{34}^A$	$\frac{1}{\sqrt{2}} [\phi^{MSMS} \otimes (\chi^{SA} \pm \chi^{AS})] \delta_{12}^S \delta_{34}^A$	$\frac{1}{\sqrt{2}} [\phi^{MSMS} \otimes (\chi^{SA} \pm \chi^{AS})] \delta_{12}^S \delta_{34}^A$
$\frac{1}{\sqrt{2}} [\phi^{SS} \otimes (\chi^{MSA} \pm \chi^{AMS})] \delta_{12}^S \delta_{34}^A$	$\frac{1}{\sqrt{2}} [\phi^{AA} \otimes (\chi^{MSA} \pm \chi^{AMS})] \delta_{12}^A \delta_{34}^A$	$\frac{1}{\sqrt{2}} [\phi^{MSMS} \otimes (\chi^{MSA} \pm \chi^{AMS})] \delta_{12}^S \delta_{34}^A$	$\frac{1}{\sqrt{2}} [\phi^{MSMS} \otimes (\chi^{MSA} \pm \chi^{AMS})] \delta_{12}^S \delta_{34}^A$
$\frac{1}{\sqrt{2}} [\phi^{SS} \otimes (\chi^{SMS} \pm \chi^{MSS})] \delta_{12}^S \delta_{34}^A$	$\frac{1}{\sqrt{2}} [\phi^{AA} \otimes (\chi^{SMS} \pm \chi^{MSS})] \delta_{12}^A \delta_{34}^A$	$\frac{1}{\sqrt{2}} [\phi^{MSMS} \otimes (\chi^{SMS} \pm \chi^{MSS})] \delta_{12}^S \delta_{34}^A$	$\frac{1}{\sqrt{2}} [\phi^{MSMS} \otimes (\chi^{SMS} \pm \chi^{MSS})] \delta_{12}^S \delta_{34}^A$
$\frac{1}{\sqrt{2}} [\phi^{SS} \otimes (\chi^{MSA} \pm \chi^{AMS})] \delta_{12}^S \delta_{34}^A$	$\frac{1}{\sqrt{2}} [\phi^{AA} \otimes (\chi^{MSA} \pm \chi^{AMS})] \delta_{12}^A \delta_{34}^A$	$\frac{1}{\sqrt{2}} [\phi^{MSMS} \otimes (\chi^{MSA} \pm \chi^{AMS})] \delta_{12}^S \delta_{34}^A$	$\frac{1}{\sqrt{2}} [\phi^{MSMS} \otimes (\chi^{MSA} \pm \chi^{AMS})] \delta_{12}^S \delta_{34}^A$
$\frac{1}{\sqrt{2}} [\phi^{SS} \otimes (\chi^{AMS} \pm \chi^{MSA})] \delta_{12}^S \delta_{34}^A$	$\frac{1}{\sqrt{2}} [\phi^{AA} \otimes (\chi^{AMS} \pm \chi^{MSA})] \delta_{12}^A \delta_{34}^A$	$\frac{1}{\sqrt{2}} [\phi^{MSMS} \otimes (\chi^{AMS} \pm \chi^{MSA})] \delta_{12}^S \delta_{34}^A$	$\frac{1}{\sqrt{2}} [\phi^{MSMS} \otimes (\chi^{AMS} \pm \chi^{MSA})] \delta_{12}^S \delta_{34}^A$
Different classes of the hidden-charm hexaquark system			
$\delta_{12}^A = 1, \delta_{34}^A = 1, \delta_{12}^S = 0, \delta_{34}^S = 0 :$	$(mn)^{I=1} c(\bar{n}\bar{n})^{I=1} \bar{c}, (mn)^{I=0} c(\bar{n}\bar{n})^{I=1} \bar{c}, (mn)^{I=0} c(\bar{n}\bar{n})^{I=0} \bar{c}$	$\delta_{12}^A = 0, \delta_{34}^A = 1, \delta_{12}^S = 1, \delta_{34}^S = 0 :$	$\delta_{12}^A = 1, \delta_{34}^A = 1, \delta_{12}^S = 1, \delta_{34}^S = 0 :$
$\delta_{12}^A = 0, \delta_{34}^A = 0, \delta_{12}^S = 1, \delta_{34}^S = 1 :$	$(mn)^{I=0} c(\bar{n}\bar{n})^{I=0} \bar{c}$	$nsc(\bar{n}\bar{n})^{I=1} \bar{c}, nsc(\bar{n}\bar{n})^{I=0} \bar{c}$	$nsc(\bar{n}\bar{n})^{I=0} \bar{c}$
$\delta_{12}^A = 1, \delta_{34}^A = 0, \delta_{12}^S = 1, \delta_{34}^S = 1 :$	$nsc(\bar{n}\bar{n})^{I=0} \bar{c}$	$\delta_{12}^A = 1, \delta_{34}^A = 1, \delta_{12}^S = 1, \delta_{34}^S = 1 :$	$\delta_{12}^A = 1, \delta_{34}^A = 1, \delta_{12}^S = 1, \delta_{34}^S = 1 :$

spin3, spin4, and spin5 represent the spins of $q_1 q_2$, $\bar{q}_3 \bar{q}_4$, $q_1 q_2 c$, $\bar{q}_3 \bar{q}_4 \bar{c}$, and the total spin, respectively.

Considering the Pauli principle, we obtain 54 types of total wave functions and present them in the first part of Table IV. Some wave functions are the eigenstates of C parity like $[\phi^{SS} \otimes \chi^{SS}]$, but others are not. For the neutral states, we need do linear superposition to construct eigen wave functions of C parity, and present them in the second part of Table IV. We introduce notations δ_{12}^A , δ_{12}^S , δ_{34}^A , and δ_{34}^S . When the two light quarks or antiquarks are antisymmetric (symmetric) in the flavor space, $\delta_{12}^A = 0$ ($\delta_{12}^S = 0$), or else $\delta_{12}^A = 1$ ($\delta_{12}^S = 1$). The hidden-charm hexaquark states can be categorized into 6 classes, and we present them in the third part of Table IV.

IV. NUMERICAL RESULTS AND DISCUSSION

Sandwiching the CMI Hamiltonian between the two wave functions with the same quantum number, we obtain the Hamiltonian matrices. Based on the corresponding eigenvalues and eigenvectors, we discuss the mass gaps, stabilities, and strong decay behaviors of all the hidden-charm hexaquark states.

From the eigenvalues, we present the mass spectra in Fig. 1 (for $nn\bar{n}\bar{n}\bar{c}$, $ss\bar{s}\bar{s}\bar{c}$, and $nnc\bar{s}\bar{s}\bar{c}$), Fig. 2 (for $nnc\bar{n}\bar{s}\bar{c}$ and $nsc\bar{n}\bar{s}\bar{c}$), and Fig. 3 (for $nsc\bar{s}\bar{s}\bar{c}$). Moreover, we also plot the corresponding thresholds which they can decay to through quark rearrangements. In convenience, we label the spin (isospin) of the rearrangement decay channel in the superscript (subscript).

In addition to the mass spectra, we discuss the two body strong decay based on the obtained eigenvectors. According to Tables III and IV, we can find that there are overlaps between hexaquark states and particular baryon-antibaryon states. In the $qqc \otimes \bar{q}\bar{q}\bar{c}$ configuration, the color wave function of the hexaquark states falls into three categories: $|(qqc)^{1_c}(\bar{q}\bar{q}\bar{c})^{1_c}\rangle$, $|(qqc)^{8_c}(\bar{q}\bar{q}\bar{c})^{8_c}\rangle$, and $|(qqc)^{10_c}(\bar{q}\bar{q}\bar{c})^{\overline{10}_c}\rangle$. The $|(qqc)^{1_c}(\bar{q}\bar{q}\bar{c})^{1_c}\rangle$ can easily dissociate into an S-wave baryon and S-wave antibaryon (the “OZI-superallowed” decay mode). In contrast, the $|(qqc)^{8_c}(\bar{q}\bar{q}\bar{c})^{8_c}\rangle$ and $|(qqc)^{10_c}(\bar{q}\bar{q}\bar{c})^{\overline{10}_c}\rangle$ fall apart through the gluon exchange. For simplicity, we only focus on the “OZI-superallowed” decay mode.

The partial width of the two body L -wave “OZI-superallowed decay” mode reads [86–88]

$$\Gamma_i = \gamma_i \alpha \frac{k^{2L+1}}{m^{2L}} \cdot |c_i|^2, \quad (7)$$

where α is an effective coupling constant, m is the initial state mass, k is the spatial momentum of the final state in the center-of-mass frame, and c_i is overlap between the hexaquark states and the final baryon-antibaryon states. Generally, γ_i depends on the spatial wave functions of the initial hexaquark and final baryon-antibaryon, which are

different for each decay process. In the heavy quark limit, $\Sigma_c (\Xi_c^*)$ and $\Sigma_c^* (\Xi_c')$ have the same spatial wave function. Based on these, we assume the γ_i relationships for different hidden-charm hexaquark states presented in Table V. We find that the $(k/m)^2$ is of $\mathcal{O}(10^{-2})$ or even smaller, which means that the large partial wave decays are all suppressed. Thus we only need to consider the S -wave two body decay modes. Employing the eigenvectors in Table VI, we calculate the values of $k \cdot |c_i|^2$ for each decay process and present them in Table VII. The blank area in Tables VI and VII means that the hexaquark state is forbidden to decay through this channel because of the quantum number conservation. According to the γ_i relationships in Table V and the values of $k \cdot |c_i|^2$ in Table VII, we can roughly estimate the relative decay widths for different two-body decay processes of a hexaquark state.

A. The $nn\bar{n}\bar{n}\bar{c}$ subsystem

Firstly, we discuss the $nn\bar{n}\bar{n}\bar{c}$ subsystem based on Fig. 1(a). They have the same mass range as the excited states of $c\bar{c}$. The $nn\bar{n}\bar{n}\bar{c}$ subsystem can be divided into three situations: $(nn)^{I=1}c(\bar{n}\bar{n})^{I=1}\bar{c}$, $(nn)^{I=0}c(\bar{n}\bar{n})^{I=1}\bar{c}$, and $(nn)^{I=0}c(\bar{n}\bar{n})^{I=0}\bar{c}$.

As for $(nn)^{I=1}c(\bar{n}\bar{n})^{I=0}\bar{c}$ states, they are antiparticles of the $(nn)^{I=0}c(\bar{n}\bar{n})^{I=1}\bar{c}$ states, thus they have the same mass spectra. We find no relative “stable” states for the $nn\bar{n}\bar{n}\bar{c}$ system, that is, all of them can decay in S -wave through strong interaction.

There are some hexaquark states which have the same quantum numbers among $(nn)^{I=1}c(\bar{n}\bar{n})^{I=1}\bar{c}$, $(nn)^{I=0}c(\bar{n}\bar{n})^{I=1}\bar{c}$, and $(nn)^{I=0}c(\bar{n}\bar{n})^{I=0}\bar{c}$. For example, both $(nn)^{I=1}c(\bar{n}\bar{n})^{I=1}\bar{c}$ and $(nn)^{I=0}c(\bar{n}\bar{n})^{I=1}\bar{c}$ have some states with the total isospin $I = 1$. The mass spectrum of these states should have been mixed, but all of the transition matrix elements of CMI Hamiltonian are zero and thus they cannot be mixed under the CMI model. According to Fig. 1(a), the masses of $(nn)^{I=1}c(\bar{n}\bar{n})^{I=1}\bar{c}$ states are usually larger than those of $(nn)^{I=0}c(\bar{n}\bar{n})^{I=1}\bar{c}$ states which are generally larger than those of $(nn)^{I=0}c(\bar{n}\bar{n})^{I=0}\bar{c}$ states. In the conventional baryon sectors, the $I = 1$ one is usually heavier than the $I = 0$ one, for example, see [$\Sigma(1189)(I=1)$ vs $\Lambda(1116)(I=0)$] and [$\Sigma_c(2455)(I=1)$ vs $\Lambda_c(2286)(I=0)$]. In our work, the wave functions of hexaquark states can be regarded as “baryon \otimes antibaryon” configuration. These two factors may result into that the hexaquark with larger isospin is heavier than that with smaller isospin. The similar results can be found in Refs. [69,85,86].

The total isospin of $(nn)^{I=1}c(\bar{n}\bar{n})^{I=1}\bar{c}$ states can be $I = 2$, 1 , and 0 . Note that the symmetry property of $(nn)^{I=1}c(\bar{n}\bar{n})^{I=1}\bar{c}$ is determined from I_{nn} and $I_{\bar{n}\bar{n}}$. Thus, the $(nn)^{I=1}c(\bar{n}\bar{n})^{I=1}\bar{c}$ states are degenerate for the total isospin of $I = 2$, 1 , and 0 in the CMI model.

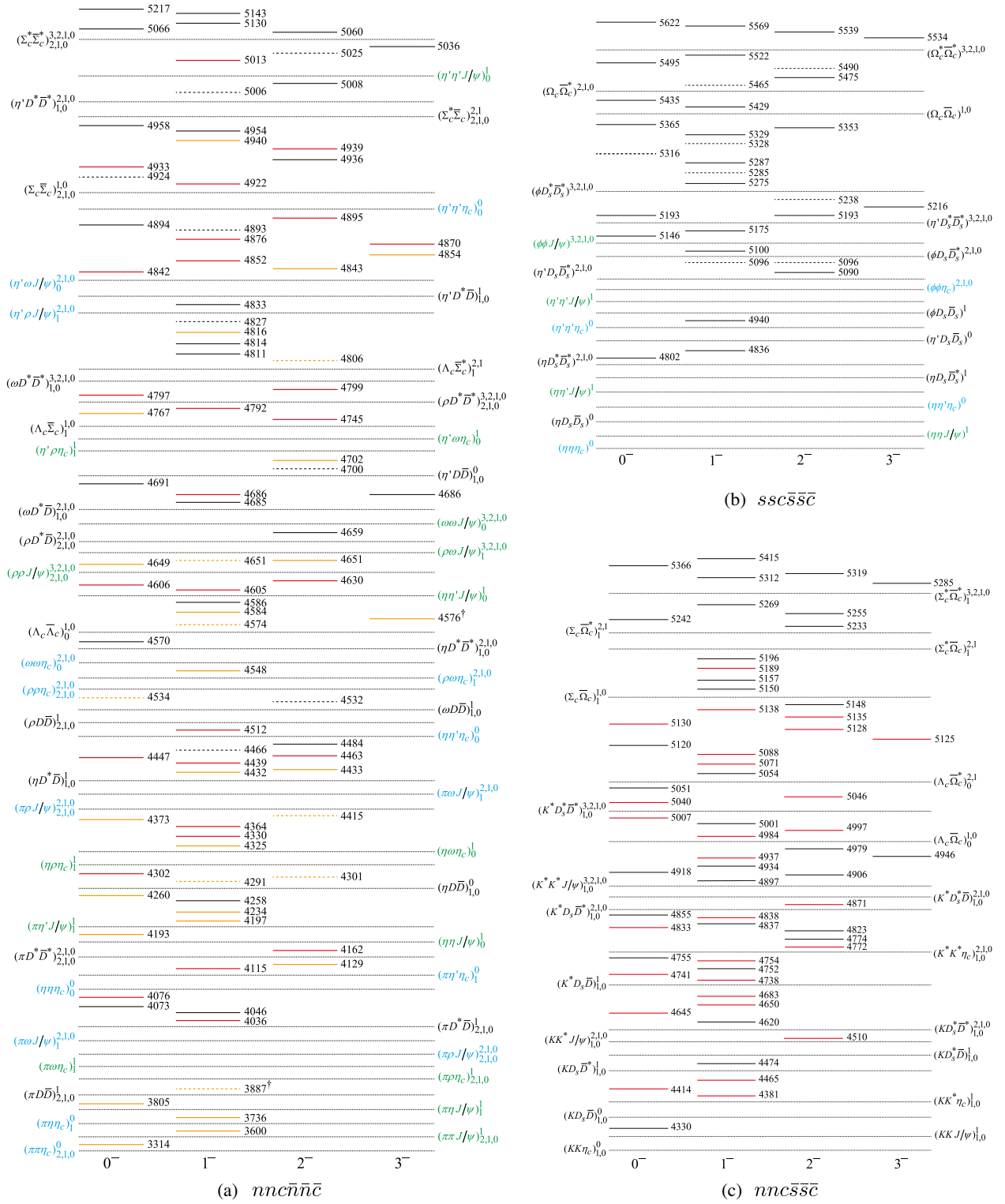


FIG. 1. Relative positions (units: MeV) for three kinds of hexaquark states. In the $nnc\bar{n}\bar{n}\bar{c}$ subsystem, the black lines show the $(nn)^{I=1}c(\bar{n}\bar{n})^{I=1}\bar{c}$ hexaquark states, the red lines show the $(nn)^{I=0}c(\bar{n}\bar{n})^{I=1}\bar{c}$ hexaquark states, and the orange lines show the $(nn)^{I=0}c(\bar{n}\bar{n})^{I=0}\bar{c}$ hexaquark states. The solid and dashed short lines are to differentiate the positive and negative C parity and it's the same as $ssc\bar{s}\bar{s}\bar{c}$ subsystem. In the $nnc\bar{s}\bar{s}\bar{c}$ subsystem, the black (red) lines represent the $nnc\bar{s}\bar{s}\bar{c}$ hexaquark states with $I = 1(0)$. The dotted lines denote various baryon-antibaryon or meson-meson-meson thresholds. Some meson-meson-meson thresholds have specific C parity, we label thresholds which have positive (negative) C parity with blue (green). When the spin (isospin) of an initial hexaquark state is equal to the number in the superscript (subscript) of a baryon-antibaryon (meson-meson-meson) state, it can decay into these state through the S -wave. Moreover, the stable states are marked with “ \dagger ”.



FIG. 2. Relative positions (units: MeV) for the $nsc\bar{n}\bar{c}$ and $nsc\bar{s}\bar{c}$ hexaquark states labeled with solid lines. In the $nsc\bar{n}\bar{c}$ subsystem, the black (red) lines represent the $nsc\bar{n}\bar{c}$ hexaquark states with $I_{j\bar{n}} = 1(0)$. In the $nsc\bar{s}\bar{c}$ subsystem, the solid (dashed) lines represent the $nsc\bar{s}\bar{c}$ hexaquark states with the positive (negative) C parity. See the caption of Fig. 1 for meaning of thresholds and “+”.

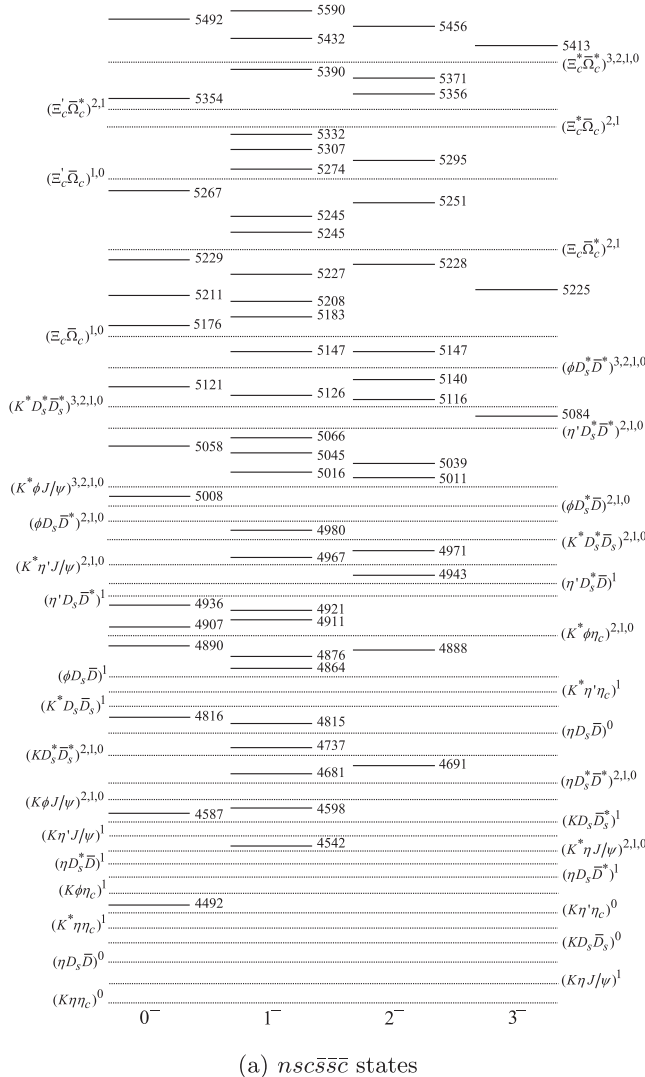


FIG. 3. Relative positions (units: MeV) for the $nsc\bar{s}\bar{s}c$ hexaquark states labeled with solid short lines. The dotted lines denote various baryon-antibaryon and meson-meson-meson thresholds. When the spin of an initial hexaquark state is equal to a number in the superscript of a baryon-antibaryon (meson-meson-meson) state, it can decay into these states through S-wave.

There are some $nnc\bar{n}\bar{n}c$ neutral states with exotic quantum numbers $J^{PC} = 0^{--}$, 1^{-+} , and 3^{-+} which the traditional mesons ($q\bar{q}$) cannot have. These exotic quantum number can help identify hidden-charm hexaquark states.

The notation $H_{n^2\bar{n}^2}(5036, 2^-, 3^{--})$ is for a hexaquark state $nnc\bar{n}\bar{n}c$ with mass around 5036 MeV and $I^G(J^{PC}) = 2^-(3^{--})$. According to the Table VI, the overlap between $H_{n^2\bar{n}^2}(5036, 2^-, 3^{--})$ and $\Sigma_c^*\bar{\Sigma}_c^*$ states is nearly 1, and thus the hexaquark is mainly made of a baryon and an antibaryon. It may behave like the ordinary scattering state if the inner interaction is not strong, but could also be a resonance or bound state dynamically generated by the baryon and antibaryon. The $H_{n^2\bar{n}^2}(5060, 2^+, 2^{+-})$,

TABLE V. The γ_i relationships for different hidden-charm hexaquark subsystems.

Subsystem	γ_i
$nnc\bar{n}\bar{n}c$	$\gamma_{\Sigma_c^*\bar{\Sigma}_c^*} = \gamma_{\Sigma_c^*\bar{\Sigma}_c} = \gamma_{\Sigma_c\bar{\Sigma}_c} = \gamma_{\Sigma_c\bar{\Sigma}_c} \gamma_{\Sigma_c\bar{\Lambda}_c} = \gamma_{\Sigma_c\bar{\Lambda}_c}$
$nsc\bar{n}\bar{s}c$	$\gamma_{\Xi_c^*\bar{\Xi}_c^*} = \gamma_{\Xi_c^*\bar{\Xi}_c} = \gamma_{\Xi_c\bar{\Xi}_c} \approx \gamma_{\Xi_c\bar{\Xi}_c} = \gamma_{\Xi_c\bar{\Xi}_c}$
$nsc\bar{n}\bar{n}c$	$\gamma_{\Xi_c^*\bar{\Sigma}_c^*} = \gamma_{\Xi_c^*\bar{\Sigma}_c} = \gamma_{\Xi_c^*\bar{\Sigma}_c} = \gamma_{\Xi_c\bar{\Sigma}_c} = \gamma_{\Xi_c\bar{\Sigma}_c}$
$nnc\bar{s}\bar{s}c$	$\gamma_{\Sigma_c^*\bar{\Omega}_c^*} = \gamma_{\Sigma_c^*\bar{\Omega}_c} = \gamma_{\Sigma_c\bar{\Omega}_c} \gamma_{\Lambda_c\bar{\Omega}_c^*} = \gamma_{\Lambda_c\bar{\Omega}_c}$
$nsc\bar{s}\bar{s}c$	$\gamma_{\Xi_c^*\bar{\Omega}_c^*} = \gamma_{\Xi_c^*\bar{\Omega}_c} = \gamma_{\Xi_c\bar{\Omega}_c} \approx \gamma_{\Xi_c\bar{\Omega}_c^*} = \gamma_{\Xi_c\bar{\Omega}_c}$
$ssc\bar{s}\bar{s}c$	$\gamma_{\Omega_c^*\bar{\Omega}_c^*} = \gamma_{\Omega_c^*\bar{\Omega}_c} = \gamma_{\Omega_c\bar{\Omega}_c} = \gamma_{\Omega_c\bar{\Omega}_c}$

$H_{n^2\bar{n}^2}(5066, 2^+, 0^{+-})$, and others have similar situations. These kinds of hexaquarks deserve a more careful study.

The $nnc\bar{n}\bar{n}c$ subsystem has one rearrangement decay mode: $nnc - \bar{n}\bar{n}c$. The $(nn)^{I=0}c(\bar{n}\bar{n})^{I=1}\bar{c}$ hexaquark states can decay to $\Lambda_c\bar{\Sigma}_c^*$ and $\Lambda_c\bar{\Sigma}_c$, but the $J^P = 2^- (0^-)$ states can only decay into $\Lambda_c\bar{\Sigma}_c^*$ ($\Lambda_c\bar{\Sigma}_c$) due to the angular momentum conservation. The $(nn)^{I=0}c(\bar{n}\bar{n})^{I=0}\bar{c}$ hexaquarks have only one decay channel $\Lambda_c\bar{\Lambda}_c$ while the $(nn)^{I=1}c(\bar{n}\bar{n})^{I=1}\bar{c}$ hexaquark states decay to $\Sigma_c^{(*)}\bar{\Sigma}_c^{(*)}$ in the “OZI-superallowed” decay mode.

One can extract the decay width information from Table VII. The $H_{n^2\bar{n}^2}(5143, 2^-, 1^{--})$ and $H_{n^2\bar{n}^2}(5130, 2^-, 1^{--})$ decay to all possible channel, but their partial width ratios are different. For the $H_{n^2\bar{n}^2}(5143, 2^-, 1^{--})$,

$$\Gamma_{\Sigma_c^*\bar{\Sigma}_c^*} : \Gamma_{(\Sigma_c^*\bar{\Sigma}_c)^-} : \Gamma_{\Sigma_c\bar{\Sigma}_c} = 2.7 : 1.6 : 1, \quad (8)$$

and for $H_{n^2\bar{n}^2}(5130, 2^-, 1^{--})$.

$$\Gamma_{\Sigma_c^*\bar{\Sigma}_c^*} : \Gamma_{(\Sigma_c^*\bar{\Sigma}_c)^-} : \Gamma_{\Sigma_c\bar{\Sigma}_c} = 7.4 : 11.5 : 1, \quad (9)$$

where $(\Sigma_c^*\bar{\Sigma}_c)^-$ is short for the $(\Sigma_c^*\bar{\Sigma}_c - \Sigma_c\bar{\Sigma}_c)/\sqrt{2}$ mode with $C = -1$.

B. The $ssc\bar{s}\bar{s}c$ subsystem

The $ssc\bar{s}\bar{s}c$ states can be considered as pure neutral particles. Some of them have normal quantum numbers $J^{PC} = 0^{--}, 1^{--}, 2^{+-}, 2^{--}$, and 3^{--} , but others carry exotic quantum numbers $J^{PC} = 0^{--}, 1^{+-}$, and 3^{-+} . Meanwhile, all of these have many different rearrangement decay channels according to Fig. 1(b) and thus their widths are relative broad.

For the two-body strong decay behaviors of the $ssc\bar{s}\bar{s}c$ subsystem, the heaviest $H_{s^2\bar{s}^2}(5651, 0^+, 0^{+-})$ has two decay modes,

$$\Gamma_{\Omega_c^*\bar{\Omega}_c^*} : \Gamma_{\Omega_c\bar{\Omega}_c} = 7.4 : 1, \quad (10)$$

and its dominant decay mode is $\Omega_c^*\bar{\Omega}_c^*$. The $H_{s^2\bar{s}^2}(5569, 0^-, 1^{--})$ state can decay through all possible baryon-antibaryon channels, and

TABLE VI. The values of eigenvectors for the $nn\bar{n}\bar{n}\bar{c}$, $nsc\bar{n}\bar{n}\bar{c}$, $nn\bar{s}\bar{s}\bar{c}$, $nsc\bar{s}\bar{s}\bar{c}$, $nsc\bar{s}\bar{s}\bar{c}$, and $ssc\bar{s}\bar{s}\bar{c}$ hexaquark subsystems. The masses are all in units of MeV.

$ss\bar{s}\bar{s}\bar{c}$ ($I = 0$)				$(nn)^{I=1}c\bar{s}\bar{s}\bar{c}$ ($I = 1$)				$(nn)^{I=1}c(\bar{n}\bar{n})^{I=1}\bar{c}$ ($I = 2, 1, 0$)				$(nn)^{I=0}c(\bar{n}\bar{n})^{I=1}\bar{c}$ ($I = 1$)								
J^{PC}	Mass	$\Omega_c^*\bar{\Omega}_c^*$	$\Omega_c^*\bar{\Omega}_c^*$	J^{PC}	Mass	$\Sigma_c^*\bar{\Omega}_c^*$	$\Sigma_c^*\bar{\Omega}_c^*$	J^{PC}	Mass	$\Sigma_c^*\bar{\Sigma}_c^*$	$\Sigma_c^*\bar{\Sigma}_c^*$	$\Sigma_c^*\bar{\Sigma}_c^*$	J^{PC}	Mass	$\Lambda_c\bar{\Sigma}_c^*$	$\Lambda_c\bar{\Sigma}_c^*$				
3 ⁻⁺	5534	-0.993		3 ⁻	5285	-0.991		3 ⁻	5036	-0.989			2 ⁻	4939	0.259					
2 ⁻⁺	5490	0.665	-0.665	2 ⁻	5319	-0.884	-0.306	-0.128	2 ⁻	5025	0.909			4895	-0.764					
2 ⁺⁺	5539	-0.983	-0.050	-0.050	5255	-0.288	0.358	0.720	2 ⁺	5060	-0.924	-0.161	-0.161	1 ⁻	5013	0.221	-0.015			
	5475	0.091	-0.664	-0.664	5233	-0.259	0.825	-0.441		5008	0.296	-0.484	-0.484		4922	0.456	0.255			
1 ⁻⁻	5569	0.918	0.135	-0.135	0.133	5415	0.688	0.3	0.275	0.188	5143	0.672	0.327	-0.327	0.338	4876	-0.634	-0.300		
	5522	-0.225	0.593	-0.593	0.248	5312	0.417	-0.116	-0.685	-0.213	5130	-0.538	0.416	-0.416	0.161	4852	-0.354	0.740		
	5429	0.087	0.243	-0.243	-0.882	5269	-0.307	0.805	-0.191	-0.169	4954	-0.217	-0.415	0.415	0.825	4792	0.128	-0.264		
1 ⁺⁻	5465	0.699	0.699		5196	-0.071	0.123	-0.439	0.774	1 ⁺	5006	0.650	0.650			4686	0.188	-0.031		
0 ⁺⁻	5622	-0.806		-0.235	5157	0.058	-0.173	-0.145	-0.284	0 ⁺	5217	-0.704		-0.369		4605	-0.191	0.097		
	5495	0.447		-0.641	5150	0.308	0.244	0.067	-0.227	5066	0.531		-0.599		0 ⁻	4933	0.118			
	5435	-0.017		0.365	0 ⁻	5366	-0.899		-0.169	4958	0.055		0.213			4842	-0.599			
						5242	0.191		-0.827						4797	0.674				
$nsc\bar{n}\bar{s}\bar{c}$ ($I = 1, 0$)				$(nsc\bar{n}\bar{n})^{I=1}\bar{c}$ ($I = 3/2, 1/2$)				$(nn)^{I=0}c(\bar{n}\bar{n})^{I=0}\bar{c}$ ($I = 0$)				$(nn)^{I=0}c(\bar{n}\bar{n})^{I=0}\bar{c}$ ($I = 0$)								
J^{PC}	Mass	$\Xi_c^*\bar{\Xi}_c^*$	$\Xi_c^*\bar{\Xi}_c'$	$\Xi_c^*\bar{\Xi}_c^*$	$\Xi_c^*\bar{\Xi}_c$	$\Xi_c^*\bar{\Xi}_c^*$	$\Xi_c^*\bar{\Xi}_c'$	$\Xi_c^*\bar{\Xi}_c^*$	J^{PC}	Mass	$\Xi_c^*\bar{\Sigma}_c^*$	$\Xi_c^*\bar{\Sigma}_c$	$\Xi_c^*\bar{\Sigma}_c^*$	J^{PC}	Mass	$\Lambda_c\bar{\Lambda}_c$				
3 ⁻⁺	5292	-0.991			3 ⁻	5164	0.989			3 ⁻	5164	0.989			1 ⁻⁻	4940	-0.319			
2 ⁺⁺	5329	-0.883	-0.148	-0.148	-0.132	5240	0.264	-0.645	-0.645	-0.095	5240	0.749	0.187	0.377	0.252	4816	-0.019			
	5240	-0.264	-0.645	-0.645	-0.095	5216	-0.303	-0.013	-0.013	0.291	5216	-0.482	0.709	0.354	0.145	4584	-0.818			
	5168	-0.064	-0.168	-0.168	0.535	5168	-0.276	-0.554	-0.705	-0.005	5116	0.203	0.140	-0.013	-0.707	0 ⁺	4767	0.562		
	5125	-0.030	0.081	0.081	-0.006	5071	-0.014	0.118	0.350	-0.345	5051	-0.014	0.118	0.350	-0.345	4649	-0.619			
2 ⁻⁻	5295	0.603	-0.603	0.131	5200	-0.026	0.026	-0.443	0.443	1 ⁻	5017	0.080	0.180	0.156	-0.293	2 ⁻	5192	-0.061		
	5155	0.218	-0.218	-0.407	0.407	5224	-0.578	-0.578	0.069	0.069	5235	-0.523	0.549	-0.036	0.067	5015	0.746			
1 ⁺⁻	5326	0.347	0.347	0.194	0.194	5224	-0.578	-0.578	0.069	0.108	5185	-0.337	-0.092	0.652	0.009	4971	-0.359			
	5134	0.066	0.066	-0.620	-0.620	5134	0.066	-0.620	-0.620	0.132	5120	-0.18	-0.042	-0.302	0.366	1 ⁻	5447	0.037	-0.023	-0.010
	5110	0.025	0.025	-0.157	-0.157	5110	0.025	-0.157	-0.291	-0.291	5090	-0.201	-0.555	0.218	0.154	5028	0.409	-0.060	-0.009	
	5066	0.101	0.101	-0.003	-0.003	5066	-0.101	0.101	-0.003	-0.440	5056	0.016	0.172	0.119	-0.591	5005	0.659	0.443	0.164	
1 ⁻⁻	5421	0.433	0.346	0.128	-0.128	5036	-0.175	0.022	0.033	-0.189	5036	-0.175	0.022	0.033	-0.189	4943	-0.426	0.634	0.025	
	5398	0.558	-0.053	0.053	0.066	5008	0.113	0.019	0.192	0.313	5008	0.113	0.019	0.192	0.313	4913	0.028	-0.033	0.078	
	5288	-0.537	0.388	-0.388	0.088	4991	0.101	0.002	-0.008	-0.302	4991	0.101	0.002	-0.008	-0.302	4896	0.171	0.215	0.432	
	5206	0.240	0.361	-0.361	-0.131	5130	-0.163	0.070	0.021	-0.108	4970	0.160	-0.163	0.070	0.021	4870	0.097	0.009	-0.588	
	5153	0.118	0.090	-0.090	-0.549	5153	-0.168	0.165	-0.211	0.204	4946	-0.168	0.165	-0.211	0.204	4822	0.017	-0.014	-0.279	
	5114	-0.065	-0.057	0.057	-0.265	5114	-0.065	0.057	-0.265	0.488	5114	-0.065	0.057	-0.265	0.488	4809	-0.226	0.017	-0.272	
	5073	0.182	-0.173	0.173	0.127	5073	0.182	-0.173	0.127	0.063	5151	0.333		-0.723	-0.049	4770	0.058	0.127	0.107	
	5050	-0.167	0.008	-0.008	0.109	5050	-0.167	0.008	-0.008	0.109	5071	-0.003		0.287	0.244	0 ⁻	5027	0.047	-0.124	
	5041	0.008	0.004	-0.004	-0.001	5041	0.008	0.004	-0.008	-0.008	5024	0.057		0.064	-0.719	4996	-0.544	-0.224		
	5027	0.093	0.067	-0.067	0.111	5027	0.093	0.067	-0.111	0.083	5015	0.018		-0.272	0.167	4914	-0.705	0.246		
	5021	-0.009	0.028	-0.028	-0.006	5021	-0.009	0.028	-0.082	0.082	4962	0.033		0.171	-0.139	4894	0.087	0.639		
	5003	0.001	-0.019	0.019	-0.124	5003	0.001	-0.019	0.019	-0.296	5003	0.001	-0.019	0.019	-0.296	4815	0.145	0.296		
	4987	-0.059	-0.030	0.030	0.046	4987	-0.059	-0.030	0.030	-0.127	4978	0.047	-0.028	0.002	-0.227	4805	-0.226	0.017	-0.272	
	4978	0.047	0.028	-0.028	-0.002	4978	0.047	0.028	-0.028	-0.002	4978	0.047	0.028	-0.028	-0.002	4805	-0.226	0.017	-0.272	
0 ⁺⁻	5407	-0.854			5407	-0.094	-0.094	-0.233	-0.112	5407	-0.094	-0.094	-0.233	-0.112	5135	0.412				
	5300	-0.064			5300	-0.052	-0.052	0.342	0.027	5300	-0.052	-0.052	0.342	0.027	5128	-0.661				
	5235	0.323			5235	-0.165	-0.165	-0.732	-0.137	5235	-0.165	-0.165	-0.732	-0.137	5189	-0.337	-0.068			
	5131	0.094			5131	-0.541	-0.541	0.309	-0.177	5131	-0.541	-0.541	0.309	-0.177	5138	-0.478	-0.225			
	5116	0.018			5116	0.030	0.030	-0.016	-0.264	5116	0.030	0.030	-0.016	-0.264	5307	-0.003	-0.202	0.184		
	5047	-0.071			5047	-0.202	-0.202	-0.175	0.733	5047	-0.202	-0.202	-0.175	0.733	5274	0.015	0.068	-0.176		
	5009	0.019			5009	-0.216	-0.216	0.092	-0.042	5009	-0.216	-0.216	0.092	-0.042	5245	-0.001	0.106	0.068		
	4976	0.041			4976	-0.052	-0.052	-0.035	0.167	4976	-0.052	-0.052	-0.035	0.167	5244	0.199	-0.119	-0.113		
0 ⁻⁻	5137				5137	0.280				5137	0.280				5227	-0.166	-0.298	-0.12		
	5117				5117	0.382				5117	0.382				5208	-0.093	0.039	-0.012		
	5084				5084	-0.441				5084	-0.441				5007	0.141	-0.151	0.186		
	5492	0.843	0.314	0.155	0.187	5492	-0.16	-0.168	-0.126	0.855	5492	0.899		0.171	0.072	0 ⁻	5211	-0.054	-0.069	-0.071
	5371	-0.437	0.629	0.551	0.147	5371	0.057	-0.134	-0.214	0.123	5371	-0.216		0.829	0.071	5176	-0.035	0.239	-0.333	
	5356	0.113	-0.611	0.735	0.0003	5356	0.023				5356	0.085		0.162	-0.710	5007	0.359			

TABLE VII. The values of $k \cdot |c_i|^2$ for the $nnc\bar{n}\bar{n}\bar{c}$, $nsc\bar{n}\bar{n}\bar{c}$, $nnc\bar{s}\bar{s}\bar{c}$, $nsc\bar{n}\bar{s}\bar{c}$, $nsc\bar{s}\bar{s}\bar{c}$, and $ssc\bar{s}\bar{s}\bar{c}$ hexaquark subsystems. The masses are all in units of MeV. The \times means that the decay channel is kinetically forbidden.

$ss\bar{s}\bar{s}\bar{c}$ ($I = 0$)						$(nn)^{I=1}c\bar{s}\bar{s}\bar{c}$ ($I = 1$)						$(nn)^{I=1}c(\bar{n}\bar{n})^{I=1}\bar{c}$ ($I = 2, 1, 0$)						$(nn)^{I=0}c(\bar{n}\bar{n})^{I=1}\bar{c}$ ($I = 1$)								
J^{PC}	Mass	$\Omega_c^*\bar{\Omega}_c^*$	$\Omega_c^*\bar{\Omega}_c$	$\Omega_c\bar{\Omega}_c^*$	$\Omega_c\bar{\Omega}_c$	J^{P}	Mass	$\Sigma_c^*\bar{\Omega}_c^*$	$\Sigma_c^*\bar{\Omega}_c$	$\Sigma_c\bar{\Omega}_c^*$	$\Sigma_c\bar{\Omega}_c$	J^{PC}	Mass	$\Sigma_c^*\bar{\Sigma}_c^*$	$\Sigma_c^*\bar{\Sigma}_c$	$\Sigma_c\bar{\Sigma}_c^*$	$\Sigma_c\bar{\Sigma}_c$	J^{P}	Mass	$\Lambda_c\bar{\Sigma}_c^*$	$\Lambda_c\bar{\Sigma}_c$					
3 ⁻⁻	5534	69				3 ⁻	5285	47				3 ⁻⁻	5036	552				2 ⁻	4939	38						
2 ⁻⁻	5490		124	124		2 ⁻	5319	238	48	9		2 ⁻⁻	5025	301					4895	272						
2 ⁺	5539	136	1	1			5255	\times	38.5	170		2 ⁺	5060	206	12	12		1 ⁻	5013	35	0.2					
	5475	\times	88	88			5233	\times	126	44			5008	\times	70	70			4922	110	59					
1 ⁻⁻	5569	271	10	10	12	1 ⁻	5415	281	65	56	30	1 ⁻⁻	5143	235	71	71	88		4876	167	76					
	5522	\times	143	143	37		5312	47	7	239	30		5130	141	109	109	19		4852	42	444					
	5429	\times	\times	\times	252		5269	\times	233	14	16		4954	\times	\times	\times	228		4792	\times	50					
1 ⁺	5465		53	53			5196	\times	\times		209	1 ⁺	5006		123	123			4686	\times	0.5					
0 ⁺	5622	325			44		5157	\times	\times		11	0 ⁺	5217	337			121		4605	\times	3					
	5495	\times		219			5150	\times	\times		2		5066	77			226		0 ⁻	4933	10					
	5435	\times			46	0 ⁻	5366	377			21		4958	\times			16		4842		178					
							5242	\times			336							4797		166						
$nsc\bar{n}\bar{s}\bar{c}$ ($I = 1, 0$)						$nsc(\bar{n}\bar{n})^{I=1}\bar{c}$ ($I = 3/2, 1/2$)						$(nn)^{I=0}c(\bar{n}\bar{n})^{I=0}\bar{c}$ ($I = 0$)						$(nn)^{I=0}c(\bar{n}\bar{n})^{I=0}\bar{c}$ ($I = 0$)								
J^{PC}	Mass	$\Xi_c^*\bar{\Xi}_c^*$	$\Xi_c^*\bar{\Xi}_c'$	$\Xi_c'\bar{\Xi}_c^*$	$\Xi_c'\bar{\Xi}_c$	$\Xi_c\bar{\Xi}_c^*$	$\Xi_c\bar{\Xi}_c'$	$\Xi_c'\bar{\Xi}_c$	$\Xi_c'\bar{\Xi}_c'$	$\Xi_c\bar{\Xi}_c$	J^{P}	Mass	$\Xi_c^*\bar{\Sigma}_c^*$	$\Xi_c^*\bar{\Sigma}_c$	$\Xi_c'\bar{\Sigma}_c^*$	$\Xi_c'\bar{\Sigma}_c$	$\Xi_c\bar{\Sigma}_c^*$	$\Xi_c\bar{\Sigma}_c$	J^{PC}	Mass	$\Lambda_c\bar{\Lambda}_c$					
3 ⁻⁻	5292	51.2									3 ⁻	5164	28.4					1 ⁻⁻	4940	95						
2 ⁺	5329	247	12	12	13	13					2 ⁻	5250	265	22	90	52			4816	0.3						
	5240	\times	88	88	5	5						5134	\times	149	39	13			4584	108						
	5216	\times	\times	\times	44	44						5116	\times	64	114	0.01		0 ⁺	4767	213						
	5168	\times	\times	\times	107	107						5071	\times	\times	\times	231			4649	160						
2 ⁻⁻	5295		317	318	12	12						5051	\times	\times	\times	48										
	5200	\times	\times	93	93							5017	\times	\times	\times	24										
	5155	\times	\times	54	54							1 ⁻	5419	213	106	85	57	68	57	2 ⁻	5192	3				
1 ⁺	5326	63	63	28	28	41	41						5235	118	179	1	4	19	10		5015	252				
	5224	17	17	3	3	8	8						5185	27	4	204	0.1	16	1	1 ⁻	4971	40				
	5134	\times	\times	88	88	9	9						5120	\times	0.4	23	78	20	0.1	1 ⁻	5447	2	1	0.1		
	5110	\times	\times	\times	\times	35	35						5090	\times	\times	\times	12	128	40		5028	82	2	0.1		
	5066	\times	\times	\times	\times	44	44						5056	\times	\times	\times	146	38	6		5005	185	116	21		
1 ⁻⁻	5421	111	88	88	15	15	12	12	84	23			5041	\times	\times	\times	6	9	9		4970	6	61	3		
	5398	167	2	2	4	4	7	7	4	1			5036	\times	\times	\times	13	9	33		4943	30	177	0.4		
	5288	\times	63	63	6	6	7	7	18	0.2			5008	\times	\times	\times	23	\times	249		4913	\times	0.4	4		
	5206	\times	\times	\times	9	9	6	6	196	5			4991	\times	\times	\times	9	\times	1		4896	\times	13	109		
	5153	\times	\times	\times	96	96	11	11	\times	13			4970	\times	\times	\times	\times	\times	0.1		4870	\times	0.01	182		
	5114	\times	\times	\times	4	4	100	100	\times	11			4946	\times	\times	\times	\times	\times	4		4822	\times	\times	31		
	5073	\times	\times	\times	\times	\times	1	1	\times	16			5114	\times	\times	\times					4809	\times	\times	27		
	5050	\times	\times	\times	\times	\times	0	0	\times	36			5151	\times							4770	\times	\times	2		
	5041	\times	\times	\times	\times	\times	\times	\times	\times	2			5071	\times				26	36	0 ⁻	5027	\times	1	13		
	5027	\times	\times	\times	\times	\times	\times	\times	\times	\times	265		5024	\times							4996	\times	169	38		
	5021	\times	\times	\times	\times	\times	\times	\times	\times	\times	1		5015	\times							4914	\times	173	38		
	5003	\times	\times	\times	\times	\times	\times	\times	\times	\times	35		4962	\times							4894	\times	2	237		
	4987	\times	\times	\times	\times	\times	\times	\times	\times	\times	8			4815	\times											
	4978	\times	\times	\times	\times	\times	\times	\times	\times	\times	1															
0 ⁺	5407	407			9	9	44	14			3 ⁻	5413	68													
	5300	1			2	2	72	1			1 ⁻	5590	216	71	88	53	45	43		2 ⁻	5135	78				
	5235	\times			19	19	245	16				5432	98	13	144	17	9	9			5128	191				
	5131	\times			136	136	\times	22				5390	\times	212	39	13	0.2	1			1 ⁻	5189	67	3		
	5116	\times			0.5	0.5	\times	47				5307	\times	\times	\times	68	91	1			5138	106	32			
	5047	\times			0.5	0.5	\times	283				5274	\times	\times	\times	9	72	23			5088	136	0.00005			
	5009	\times			3	3	\times	1				5245	\times	\times	\times	\times	15	185			5071	4	318			
	4976	\times					\times	\times	\times	9		5244	\times	\times	\times	\times	2	8			4984	\times	3			
0 ⁻⁻	5137				38	38						5227	\times	\times	\times	\times	\times	80				5040	\times	256		
	5117				62	62						5208	\times	\times	\times	\times	\times	11				5007	\times	33		
	5084				62	62						5183	\times	\times	\times	\times	\times	0.1								
												0 ⁻	5492	1		0.2	0.1	0.1	0 ⁻	5211	\times	\times	2			
	2 ⁻	5456	249	55	13	27	5295	\times	\times	\times	294		5354	\times			319		4		5176	<				

$$\Gamma_{\Omega_c^*\bar{\Omega}_c^*} : \Gamma_{(\Omega_c^*\bar{\Omega}_c)^-} : \Gamma_{\Omega_c\bar{\Omega}_c} = 22.6 : 1.7 : 1, \quad (11)$$

where the $(\Omega_c^*\bar{\Omega}_c)^-$ means $(\Omega_c^*\bar{\Omega}_c - \Omega_c\bar{\Omega}_c^*)/\sqrt{2}$ which is antisymmetric under the C -parity transformation. Moreover, for the states $H_{s^2\bar{s}^2}(5429, 0^-, 1^{--})$ and $H_{s^2\bar{s}^2}(5435, 0^+, 0^{+-})$, their masses are similar and they can only decay through $\Omega_c\bar{\Omega}_c$ mode. $H_{s^2\bar{s}^2}(5495, 0^+, 0^{+-})$ and $H_{s^2\bar{s}^2}(5490, 0^+, 2^{--})$ have similar masses but the former can decay into $\Omega_c\bar{\Omega}_c$ while the latter can decay through $(\Omega_c^*\bar{\Omega}_c - \Omega_c\bar{\Omega}_c^*)/\sqrt{2}$ in S -wave.

The rest of $ss\bar{s}\bar{s}\bar{c}$ hexaquark states are below the baryon-antibaryon decay channels. Therefore, their mainly rearrangement decay channels should be meson-meson-meson decay channels.

C. The $nnc\bar{s}\bar{s}\bar{c}$ subsystem

According to Fig. 1(c), we discuss the mass spectra and decay behavior of $nnc\bar{s}\bar{s}\bar{c}$ subsystem. For the $I = 1$ $nnc\bar{s}\bar{s}\bar{c}$ states, they are explicitly exotic states. There are still no relative stable states in $nnc\bar{s}\bar{s}\bar{c}$ subsystem.

For the $I = 0$ states, they have only two channels: $\Lambda_c\bar{\Omega}_c^*$ and $\Lambda_c\bar{\Omega}_c$. The two states $H_{n^2\bar{s}^2}(5128, 0, 2^-)$ and $H_{n^2\bar{s}^2}(5130, 0, 0^-)$ can be distinguished by their respective decay modes. The $H_{n^2\bar{s}^2}(5128, 0, 2^-)$ can dissociate into $\Lambda_c\bar{\Omega}_c^*$ while $H_{n^2\bar{s}^2}(5130, 0, 0^-)$ can decay into $\Lambda_c\bar{\Omega}_c$ in S -wave.

There are four different decay channels for the $I = 1$ states: $\Sigma_c^*\bar{\Omega}_c^*$, $\Sigma_c\bar{\Omega}_c^*$, $\Sigma_c^*\bar{\Omega}_c$, and $\Sigma_c\bar{\Omega}_c$. From Table VII, for $H_{n^2\bar{s}^2}(5415, 1, 1^-)$ state,

$$\Gamma_{\Sigma_c^*\bar{\Omega}_c^*} : \Gamma_{\Sigma_c\bar{\Omega}_c^*} : \Gamma_{\Sigma_c^*\bar{\Omega}_c} : \Gamma_{\Sigma_c\bar{\Omega}_c} = 9.4 : 2.2 : 1.9 : 1. \quad (12)$$

and for the $H_{n^2\bar{s}^2}(5312, 1, 1^-)$ state

$$\Gamma_{\Sigma_c^*\bar{\Omega}_c^*} : \Gamma_{\Sigma_c\bar{\Omega}_c^*} : \Gamma_{\Sigma_c^*\bar{\Omega}_c} : \Gamma_{\Sigma_c\bar{\Omega}_c} = 1.6 : 0.2 : 8 : 1. \quad (13)$$

D. The $nsc\bar{n}\bar{n}\bar{c}$ subsystem

We discuss the mass spectra and decay behaviors of $nsc\bar{n}\bar{n}\bar{c}$ subsystem based on Fig. 2(a). The $nnc\bar{n}\bar{s}\bar{c}$ states are antiparticles of the $nsc\bar{n}\bar{n}\bar{c}$ states, and thus they have the same mass spectra.

The $nsc\bar{n}\bar{n}\bar{c}$ subsystem can be divided into two situations: $nsc(\bar{n}\bar{n})^{I=1}\bar{c}$ and $nsc(\bar{n}\bar{n})^{I=0}\bar{c}$. For the $nsc(\bar{n}\bar{n})^{I=1}\bar{c}$ states, the mass spectra are identical for total isospin of $I = 3/2$ and $1/2$ in CMI model similar to $(nn)^{I=1}c(\bar{n}\bar{n})^{I=1}\bar{c}$ subsystem. The $nsc\bar{n}\bar{n}\bar{c}$ states with $I = 3/2$ are explicitly exotic and thus easily identifiable as candidates for the hidden-charm hexaquark state.

From Fig. 2(a), we find the lowest 0^- , 1^- , 2^- , and 3^- states are relatively stable states, and especially the $H_{ns\bar{n}^2}(3578, 1/2, 0^-)$ is below all the thresholds for rearrangement decay channels. The other three states can still decay via D -wave strong interaction. For example, the

$H_{ns\bar{n}^2}(4682, 1/2, 3^-)$ can decay into $KD^*\bar{D}$ final states via D -wave.

From Table VII, there are 6 and 3 possible baryon-antibaryon channels for the $nsc(\bar{n}\bar{n})^{I=1}\bar{c}$ and $nsc(\bar{n}\bar{n})^{I=0}\bar{c}$ subsystems, respectively. The $H_{ns\bar{n}^2}(5071, 3/2, 2^-)$ and $H_{ns\bar{n}^2}(5071, 3/2, 0^-)$ are accidentally degenerate, but the $J^P = 2^-$ state can decay into $\Xi_c^*\bar{\Sigma}_c^*$, $\Xi_c^*\bar{\Sigma}_c$, $\Xi_c'\bar{\Sigma}_c^*$, and $\Xi_c'\bar{\Sigma}_c$ while the $J^P = 0^-$ state can only decay through $\Xi_c^*\bar{\Sigma}_c^*$, and $\Xi_c\bar{\Sigma}_c$ channels. Similarly, $H_{ns\bar{n}^2}(4971, 1/2, 2^-)$ can only decay through $\Xi_c^*\bar{\Lambda}_c$ mode, but $H_{ns\bar{n}^2}(4970, 1/2, 1^-)$ can only decay into $\Xi_c'\bar{\Lambda}_c$, $\Xi_c'\bar{\Lambda}_c$ and $\Xi_c\bar{\Lambda}_c$ modes. We can distinguish $H_{ns\bar{n}^2}(4913, 1/2, 1^-)$ and $H_{ns\bar{n}^2}(4914, 1/2, 0^-)$ by partial decay width ratios since for the former,

$$\Gamma_{\Xi_c'\bar{\Lambda}_c} : \Gamma_{\Xi_c\bar{\Lambda}_c} = 0.1 : 1. \quad (14)$$

and for the latter,

$$\Gamma_{\Xi_c'\bar{\Lambda}_c} : \Gamma_{\Xi_c\bar{\Lambda}_c} = 4.6 : 1. \quad (15)$$

E. The $nsc\bar{n}\bar{s}\bar{c}$ subsystem

Here, we discuss the $nsc\bar{n}\bar{s}\bar{c}$ subsystem based on Fig. 2(b). The subsystem is also a pure neutral subsystem, thus C parity and G parity are good quantum numbers. Since there is no constraint from the Pauli principle for $nsc\bar{n}\bar{s}\bar{c}$ subsystem, the values of δ_{12}^A , δ_{12}^S , δ_{34}^A , and δ_{34}^S from Table IV are all 1 and the obtained mass spectra is more complicated than other subsystems. There are no relative stable states for the $nsc\bar{n}\bar{s}\bar{c}$ subsystem.

Similar to the $nnc\bar{n}\bar{n}\bar{c}$ states, the mass spectra of $nsc\bar{n}\bar{s}\bar{c}$ states are identical for total isospin of $I = 1$ and 0 in CMI model. From Fig. 2(b), we find nine good exotic states candidates for quantum numbers $J^{PC} = 0^{--}$.

The mass of $H_{ns\bar{n}^2}(5117, 1^-(0^+), 0^{--})$ is very closed to $H_{ns\bar{n}^2}(5114, 1^-(0^+), 1^{--})$, and they all can decay into $(\Xi_c^*\bar{\Xi}_c - \Xi_c\bar{\Xi}_c')/\sqrt{2}$. However, the $H_{ns\bar{n}^2}(5114, 1^+(0^-), 1^{--})$ has others decay channels. From Table VII, we obtain for $H_{ns\bar{n}^2}(5114, 1^+(0^-), 1^{--})$

$$\Gamma_{(\Xi_c^*\bar{\Xi}_c)^-} : \Gamma_{(\Xi_c'\bar{\Xi}_c)^-} : \Gamma_{\Xi_c\bar{\Xi}_c} = 0.6 : 18.1 : 1, \quad (16)$$

where $(\Xi_c^*\bar{\Xi}_c)^-$ and $(\Xi_c'\bar{\Xi}_c)^-$ represent $(\Xi_c^*\bar{\Xi}_c - \Xi_c\bar{\Xi}_c^*)/\sqrt{2}$ and $(\Xi_c'\bar{\Xi}_c - \Xi_c\bar{\Xi}_c')/\sqrt{2}$ respectively.

F. The $nsc\bar{s}\bar{s}\bar{c}$ subsystem

Lastly, we discuss the mass spectra and decay behavior of $nsc\bar{s}\bar{s}\bar{c}$ subsystem based on the Fig. 3(a). The $ss\bar{n}\bar{n}\bar{c}$ states are antiparticles of the $nsc\bar{s}\bar{s}\bar{c}$ states, and thus they have the same mass spectra. The restrictions from Pauli principle for the $nsc\bar{s}\bar{s}\bar{c}$ states are the same as the $nsc(\bar{n}\bar{n})^{I=1}\bar{c}$ states, and therefore the numbers of their states are equal.

From Fig. 3(a), we easily find that there are no relative stable states. The $nsc\bar{s}\bar{s}\bar{c}$ states are higher than many

different rearrangement decay channels. Therefore, they would have a relative wide width. In conclusion, we do not suggest that the experimentalists foremost find these states.

The reference baryon-antibaryon systems for the $nsc\bar{s}\bar{s}\bar{c}$ states are the $\Xi_c^*\bar{\Omega}_c^*$, $\Xi'_c\bar{\Omega}_c^*$, $\Xi_c\bar{\Omega}_c^*$, $\Xi_c^*\bar{\Omega}_c$, $\Xi'_c\bar{\Omega}_c$, and $\Xi_c\bar{\Omega}_c$. The mass of $H_{ns\bar{s}^2}(5356, 1/2, 2^-)$ is close to that of $H_{ns\bar{s}^2}(5354, 1/2, 0^-)$. For $H_{ns\bar{s}^2}(5356, 1/2, 2^-)$ state, it can decay through $\Xi_c^*\bar{\Omega}_c^*$, $\Xi'_c\bar{\Omega}_c$, and $\Xi_c\bar{\Omega}_c$ channels. But $H_{ns\bar{s}^2}(5354, 1/2, 0^-)$ can decay into $\Xi'_c\bar{\Omega}_c$ and $\Xi_c\bar{\Omega}_c$ channels. Then we consider $H_{ns\bar{s}^2}(5245, 1/2, 2^-)$ and $H_{ns\bar{s}^2}(5244, 1/2, 2^-)$, and both of them can decay through $\Xi_c^*\bar{\Omega}_c^*$ and $\Xi_c\bar{\Omega}_c$ channels in S -wave. From Table VII, for $H_{ns\bar{s}^2}(5245, 1/2, 2^-)$,

$$\Gamma_{\Xi_c\bar{\Omega}_c^*} : \Gamma_{\Xi_c\bar{\Omega}_c} = 0.1 : 1, \quad (17)$$

and for $H_{ns\bar{s}^2}(5244, 1/2, 2^-)$,

$$\Gamma_{\Xi_c\bar{\Omega}_c^*} : \Gamma_{\Xi_c\bar{\Omega}_c} = 0.3 : 1. \quad (18)$$

V. SUMMARY

Up to now, more and more hidden-charm tetraquark states and pentaquark states have been discovered and confirmed by different experiments. These give us a significant confidence to the existence of hidden-charm hexaquark states. Thus, we studied systematically the mass spectra, stability, and strong decay behaviors of hidden-charm hexaquark states in the framework of the CMI model.

First, we introduce the CMI model and extract the corresponding coupling constants from traditional hadrons. Next, we construct the flavor \otimes color \otimes spin wave functions based on the SU(3) and SU(2) symmetry. Meanwhile, we require the wave function to obey Pauli Principle. After that, we systematically calculate the mass spectra, corresponding overlap, and the values of $k \cdot |c_i|$. Lastly, we specifically discuss the stability, the possible quark rearrangement decay channels, and the relative decay width ratios.

For $nn\bar{c}\bar{n}\bar{c}$, $ssc\bar{s}\bar{s}\bar{c}$, and $nsc\bar{n}\bar{s}\bar{c}$ subsystems, they are pure neutral particles (except $(nn)^{I=0}c(\bar{n}\bar{n})^{I=1}\bar{c}$ subsystem), and C parity and G parity both are good quantum numbers. According to the mass spectra, we find that the lower isospin quantum number, the more compact hexaquark states. Here, the $J^{PC} = 0^{--}, 1^{-+}, 3^{++}$ states are good exotic states candidates, and especially the 0^{--} states which even the S -wave tetraquark states cannot carry.

We list some possible stable hexaquark states in Table VIII. We find ten relative stable states, which are below all allowed rearrangement decay channels. These states belong to the $nn\bar{c}\bar{n}\bar{c}$ subsystem, $nsc\bar{n}\bar{n}\bar{c}$ subsystem and $nsc\bar{n}\bar{s}\bar{c}$ subsystem respectively. We think the $H_{ns\bar{n}^2}(3578, 1/2, 0^-)$ and $H_{ns\bar{n}^2}(3670, 1/2, 1^-)$ states are better stable candidates which could be first searched for in experiments.

TABLE VIII. The relatively stable states of hidden-charm hexaquark system in CMI model. The masses are all in units of MeV.

States	$I^G(J^{PC})$	Masses	States	$I^{(G)}(J^{P(C)})$	Masses
$nsc\bar{n}\bar{s}\bar{c}$	$0^+(0^{++})$	3815	$nsc\bar{n}\bar{n}\bar{c}$	$1/2(0^-)$	3578
	$0^-(1^{--})$	4005		$1/2(1^-)$	3670
	$0^-(2^{--})$	4443		$1/2(2^-)$	4090
	$1^+(2^{+-})$			$1/2(3^-)$	4682
	$0^-(3^{--})$	4794		$0^+(1^{++})$	3887
	$1^+(3^{+-})$			$0^-(3^{--})$	4576

In order to check the uncertainty of our framework, we also determine the $v_{q\bar{q}}$ and $m_{q\bar{q}}$ with the masses of pseudoscalar mesons. Since the spontaneously breaking of vacuum symmetry strongly affects the properties of these pseudoscalar mesons, the parameters of $v_{q\bar{q}}$ and $m_{q\bar{q}}$ are not the same as those obtained with the vector mesons. For example, $v_{n\bar{n}}$ and $m_{n\bar{n}}$ become 29.87 MeV and 153.99 MeV in the new scenario, respectively. However, the difference between the hexaquark masses of the two scenarios can be roughly used to estimate the uncertainty of our approach. We give the comparison of the $(nn)^{I=0}c(\bar{n}\bar{n})^{I=0}\bar{c}$ and $ssc\bar{s}\bar{s}\bar{c}$ systems with $I^G(J^{PC}) = 0^-(1^{--})$ in Table IX. Scen.1 (Scen.2) denotes the results calculated by using the parameters obtained with the vector (pseudoscalar) mesons. Firstly, one notices that the ground states differ largest from the table. The heavier the state is, the smaller the difference between the two scenarios is. These may be resulted from that the new $v_{q\bar{q}}$ becomes larger while the new $m_{q\bar{q}}$ becomes smaller. Second, the mass of the $(nn)^{I=0}c(\bar{n}\bar{n})^{I=0}\bar{c}$ ground state with $I^G(J^{PC}) = 0^-(1^{--})$ changes about 399 MeV while that for the $ssc\bar{s}\bar{s}\bar{c}$ case only varies about 166 MeV. That is, the uncertainty reduces

TABLE IX. The comparison of the masses for the $(nn)^{I=0}c(\bar{n}\bar{n})^{I=0}\bar{c}$ and $ssc\bar{s}\bar{s}\bar{c}$ systems with $I^G(J^{PC}) = 0^-(1^{--})$ in two scenarios. All masses are in units of MeV.

$nn\bar{c}\bar{n}\bar{c}$		$ssc\bar{s}\bar{s}\bar{c}$	
Scen.1	Scen.2	Scen.1	Scen.2
3600	3201	4836	4670
3736	3443	4940	4871
4197	3960	5100	5068
4234	4053	5175	5152
4325	4260	5275	5258
4432	4437	5287	5274
4548	4520	5329	5298
4584	4588	5429	5434
4816	4835	5522	5556
4940	5003	5569	5592

when the number of n/\bar{n} quark in hexaquark states decreases, which is because the mass difference between π and ρ mesons is much larger than those between K and K^* mesons.

In summary, we give a preliminary study about the mass spectra of hidden-charm hexaquark states. In addition to the CMI model, other nonperturbative QCD methods can also help us to understand more properties of the hexaquark states in detail such as QCD sum rule, effective fields theories and lattice QCD simulations. We hope that our study may inspire theorists and experimentalists to pay attention to these hidden-charm hexaquark states.

ACKNOWLEDGMENTS

This work is supported by the China National Funds for Distinguished Young Scientists under Grant No. 11825503, National Key Research and Development Program of China under Contract No. 2020YFA0406400, the 111 Project under Grant No. B20063, and the National Natural Science Foundation of China under Grant No. 12047501. This project is also supported by the National Natural Science Foundation of China under Grants No. 12175091, and 11965016, CAS Interdisciplinary Innovation Team, and the Fundamental Research Funds for the Central Universities under Grants No. Izujbky-2021-sp24.

-
- [1] S. K. Choi *et al.* (Belle Collaboration), Observation of a Narrow Charmonium-Like State in Exclusive $B^\pm \rightarrow K^\pm \pi^+ \pi^- J/\psi$ Decays, *Phys. Rev. Lett.* **91**, 262001 (2003).
 - [2] D. Acosta *et al.* (CDF Collaboration), Observation of the Narrow State $X(3872) \rightarrow J/\psi \pi^+ \pi^-$ in $\bar{p}p$ Collisions at $\sqrt{s} = 1.96$ TeV, *Phys. Rev. Lett.* **93**, 072001 (2004).
 - [3] V. M. Abazov *et al.* (D0 Collaboration), Observation and Properties of the $X(3872)$ Decaying to $J/\psi \pi^+ \pi^-$ in $p\bar{p}$ Collisions at $\sqrt{s} = 1.96$ TeV, *Phys. Rev. Lett.* **93**, 162002 (2004).
 - [4] R. Aaij *et al.* (LHCb Collaboration), Observation of the Resonant Character of the $Z(4430)^-$ State, *Phys. Rev. Lett.* **112**, 222002 (2014).
 - [5] M. Ablikim *et al.* (BESIII Collaboration), Evidence of Two Resonant Structures in $e^+e^- \rightarrow \pi^+\pi^- h_c$, *Phys. Rev. Lett.* **118**, 092002 (2017).
 - [6] M. Ablikim *et al.* (BESIII Collaboration), Precise Measurement of the $e^+e^- \rightarrow \pi^+\pi^- J/\psi$ Cross Section at Center-of-Mass Energies from 3.77 to 4.60 GeV, *Phys. Rev. Lett.* **118**, 092001 (2017).
 - [7] M. Ablikim *et al.* (BESIII Collaboration), Measurement of $e^+e^- \rightarrow \pi^+\pi^-\psi(3686)$ from 4.008 to 4.600 GeV and observation of a charged structure in the $\pi^\pm\psi(3686)$ mass spectrum, *Phys. Rev. D* **96**, 032004 (2017).
 - [8] M. Ablikim *et al.* (BESIII Collaboration), Observation of a Near-Threshold Structure in the K^+ Recoil-Mass Spectra in $e^+e^- \rightarrow K^+(D_s^- D^{*0} + D_s^{*-} D^0)$, *Phys. Rev. Lett.* **126**, 102001 (2021).
 - [9] R. Aaij *et al.* (LHCb Collaboration), Observation of $J/\psi p$ Resonances Consistent with Pentaquark States in $\Lambda_b^0 \rightarrow J/\psi K^- p$ Decays, *Phys. Rev. Lett.* **115**, 072001 (2015).
 - [10] R. Aaij *et al.* (LHCb Collaboration), Model-Independent Evidence for $J/\psi p$ Contributions to $\Lambda_b^0 \rightarrow J/\psi p K^-$ Decays, *Phys. Rev. Lett.* **117**, 082002 (2016).
 - [11] R. Aaij *et al.* (LHCb Collaboration), Observation of a Narrow Pentaquark State, $P_c(4312)^+$, and of Two-Peak Structure of the $P_c(4450)^+$, *Phys. Rev. Lett.* **122**, 222001 (2019).
 - [12] The talk by Franz Muheim at the European Physical Society conference on high energy physics 2021 on July 28, <https://indico.desy.de/event/28202/contributions/102717/>.
 - [13] G. Falldt and C. Wilkin, Estimation of the ratio of the $pn \rightarrow p n \pi^0 \pi^0 / pn \rightarrow d \pi^0 \pi^0$ cross sections, *Phys. Lett. B* **701**, 619 (2011).
 - [14] P. Adlarson *et al.* (WASA-at-COSY Collaboration), ABC Effect in Basic Double-Pionic Fusion—Observation of a New Resonance?, *Phys. Rev. Lett.* **106**, 242302 (2011).
 - [15] P. Adlarson *et al.* (WASA-at-COSY Collaboration), Isospin decomposition of the basic double-pionic fusion in the region of the ABC effect, *Phys. Lett. B* **721**, 229 (2013).
 - [16] R. L. Jaffe, Perhaps a Stable Dihyperon, *Phys. Rev. Lett.* **38**, 195 (1977).
 - [17] S. A. Yost and C. R. Nappi, The mass of the H dibaryon in a chiral model, *Phys. Rev. D* **32**, 816 (1985).
 - [18] S. D. Paganis, G. W. Hoffmann, R. L. Ray, J. L. Tang, T. Udagawa, and R. S. Longacre, Can doubly strange dibaryon resonances be discovered at RHIC?, *Phys. Rev. C* **62**, 024906 (2000).
 - [19] J. L. Rosner, SU(3) breaking and the H dibaryon, *Phys. Rev. D* **33**, 2043 (1986).
 - [20] G. Karl and P. Zenczykowski, H Dibaryon spectroscopy, *Phys. Rev. D* **36**, 2079 (1987).
 - [21] P. B. Mackenzie and H. B. Thacker, Evidence Against a Stable Dibaryon from Lattice QCD, *Phys. Rev. Lett.* **55**, 2539 (1985).
 - [22] A. T. M. Aerts and J. Rafelski, QCD, bags and hadron masses, *Phys. Lett.* **148B**, 337 (1984).
 - [23] A. P. Balachandran, A. Barducci, F. Lizzi, V. G. J. Rodgers, and A. Stern, A Doubly Strange Dibaryon in the Chiral Model, *Phys. Rev. Lett.* **52**, 887 (1984).
 - [24] U. Straub, Z. Y. Zhang, K. Brauer, A. Faessler, and S. B. Khadkikar, Binding energy of the dihyperon in the quark cluster model, *Phys. Lett. B* **200**, 241 (1988).
 - [25] M. Oka, Y. R. Liu, and W. Meguro, Charmed deuteron, *Few-Body Syst.* **54**, 1255 (2013).
 - [26] S. M. Gerasyuta and E. E. Matskevich, Heavy dibaryons, *Int. J. Mod. Phys. E* **20**, 2443 (2011).

- [27] M. Oka, S. Maeda, and Y.R. Liu, Charmed dibaryon resonances in the potential quark model, *Int. J. Mod. Phys. Conf. Ser.* **49**, 1960004 (2019).
- [28] S. Pepin and F. Stancu, Heavy hexaquarks in a chiral constituent quark model, *Phys. Rev. D* **57**, 4475 (1998).
- [29] Y.R. Liu, W. Meguro, and M. Oka, Possible molecular bound states: $\Lambda_c N$ and $\Lambda_c \Lambda_c$, *EPJ Web Conf.* **20**, 01001 (2012).
- [30] J. Vijande, A. Valcarce, J. M. Richard, and P. Sorba, Search for doubly-heavy dibaryons in a quark model, *Phys. Rev. D* **94**, 034038 (2016).
- [31] L. Meng, N. Li, and S. L. Zhu, Deuteron-like states composed of two doubly charmed baryons, *Phys. Rev. D* **95**, 114019 (2017).
- [32] Z. G. Wang, Analysis of the scalar doubly charmed hexaquark state with QCD sum rules, *Eur. Phys. J. C* **77**, 642 (2017).
- [33] W. Meguro, Y. R. Liu, and M. Oka, Possible $\Lambda_c \Lambda_c$ molecular bound state, *Phys. Lett. B* **704**, 547 (2011).
- [34] J. Leandri and B. Silvestre-Brac, Dibaryon states containing two different types of heavy quarks, *Phys. Rev. D* **51**, 3628 (1995).
- [35] N. Li and S. L. Zhu, Hadronic molecular states composed of heavy flavor baryons, *Phys. Rev. D* **86**, 014020 (2012).
- [36] Z. G. Wang, Triply-charmed hexaquark states with the QCD sum rules, *Int. J. Mod. Phys. A* **35**, 2050073 (2020).
- [37] R. Chen, F. L. Wang, A. Hosaka, and X. Liu, Exotic triple-charm deuteronlike hexaquarks, *Phys. Rev. D* **97**, 114011 (2018).
- [38] J. M. Richard, A. Valcarce, and J. Vijande, Very Heavy Flavored Dibaryons, *Phys. Rev. Lett.* **124**, 212001 (2020).
- [39] Z. Y. Zhang, Y. W. Yu, P. N. Shen, L. R. Dai, A. Faessler, and U. Straub, Hyperon nucleon interactions in a chiral SU(3) quark model, *Nucl. Phys. A* **625**, 59 (1997).
- [40] S. M. Gerasyuta and E. E. Matskevich, Hexaquarks in the coupled-channel formalism, *Phys. Rev. D* **82**, 056002 (2010).
- [41] B. Silvestre- Brac and J. Leandri, Systematics of q-6 systems in a simple chromomagnetic model, *Phys. Rev. D* **45**, 4221 (1992).
- [42] W. Park, A. Park, and S. H. Lee, Dibaryons in a constituent quark model, *Phys. Rev. D* **92**, 014037 (2015).
- [43] X. H. Chen, Q. N. Wang, W. Chen, and H. X. Chen, Exotic $\Omega\Omega$ dibaryon states in a molecular picture, *Chin. Phys. C* **45**, 041002 (2021).
- [44] M. Oka, Flavor octet dibaryons in the quark model, *Phys. Rev. D* **38**, 298 (1988).
- [45] H. Huang, J. Ping, X. Zhu, and F. Wang, Full heavy dibaryons, [arXiv:2011.00513](https://arxiv.org/abs/2011.00513).
- [46] M. Ablikim *et al.* (BESIII Collaboration), Cross section measurement of $e^+e^- \rightarrow \pi^+\pi^-(3686)$ from $\sqrt{S} = 4.0076$ to 4.6984 GeV, *Phys. Rev. D* **104**, 052012 (2021).
- [47] X. L. Wang *et al.* (Belle Collaboration), Observation of Two Resonant Structures in $e^+e^- \rightarrow \pi^+\pi^-\psi(2S)$ via Initial State Radiation at Belle, *Phys. Rev. Lett.* **99**, 142002 (2007).
- [48] X. L. Wang *et al.* (Belle Collaboration), Measurement of $e^+e^- \rightarrow \pi^+\pi^-\psi(2S)$ via initial state radiation at Belle, *Phys. Rev. D* **91**, 112007 (2015).
- [49] J. P. Lees *et al.* (BABAR Collaboration), Study of the reaction $e^+e^- \rightarrow \psi(2S)\pi^+\pi^-$ via initial-state radiation at BABAR, *Phys. Rev. D* **89**, 111103 (2014).
- [50] J. Z. Wang, R. Q. Qian, X. Liu, and T. Matsuki, Are the Y states around 4.6 GeV from e^+e^- annihilation higher charmonia?, *Phys. Rev. D* **101**, 034001 (2020).
- [51] C. F. Qiao, A uniform description of the states recently observed at B -factories, *J. Phys. G* **35**, 075008 (2008).
- [52] S. Dubynskiy and M. B. Voloshin, Hadro-charmonium, *Phys. Lett. B* **666**, 344 (2008).
- [53] G. Cotugno, R. Faccini, A. D. Polosa, and C. Sabelli, Charmed Baryonium, *Phys. Rev. Lett.* **104**, 132005 (2010).
- [54] C. F. Qiao, One explanation for the exotic state $Y(4260)$, *Phys. Lett. B* **639**, 263 (2006).
- [55] Y. D. Chen and C. F. Qiao, Baryonium study in heavy baryon chiral perturbation theory, *Phys. Rev. D* **85**, 034034 (2012).
- [56] G. Pakhlova *et al.* (Belle Collaboration), Observation of a Near-Threshold Enhancement in the $e^+e^- \rightarrow \Lambda_c^+\Lambda_c^-$ Cross Section using Initial-State Radiation, *Phys. Rev. Lett.* **101**, 172001 (2008).
- [57] N. Lee, Z. G. Luo, X. L. Chen, and S. L. Zhu, Possible deuteron-like molecular states composed of heavy baryons, *Phys. Rev. D* **84**, 014031 (2011).
- [58] Y. D. Chen, C. F. Qiao, P. N. Shen, and Z. Q. Zeng, Revisiting the spectrum of baryonium in heavy baryon chiral perturbation theory, *Phys. Rev. D* **88**, 114007 (2013).
- [59] X. Li and M. B. Voloshin, Y (4260) and Y (4360) as mixed hadrocharmonium, *Mod. Phys. Lett. A* **29**, 1450060 (2014).
- [60] S. M. Gerasyuta and E. E. Matskevich, Heavy baryonia with the open and hidden charm, *Int. J. Mod. Phys. E* **22**, 1350093 (2013).
- [61] S. M. Gerasyuta and E. E. Matskevich, Baryonia with open and hidden bottom, *Int. J. Mod. Phys. E* **29**, 2050038 (2020).
- [62] S. M. Gerasyuta and E. E. Matskevich, Baryonia with open and hidden strange, *Int. J. Mod. Phys. E* **29**, 2050035 (2020).
- [63] J. X. Lu, L. S. Geng, and M. P. Valderrama, Heavy baryon-antibaryon molecules in effective field theory, *Phys. Rev. D* **99**, 074026 (2019).
- [64] B. D. Wan, L. Tang, and C. F. Qiao, Hidden-bottom and -charm hexaquark states in QCD sum rules, *Eur. Phys. J. C* **80**, 121 (2020).
- [65] H. X. Chen, D. Zhou, W. Chen, X. Liu, and S. L. Zhu, Searching for hidden-charm baryonium signals in QCD sum rules, *Eur. Phys. J. C* **76**, 602 (2016).
- [66] A. De Rujula, H. Georgi, and S. L. Glashow, Hadron masses in a gauge theory, *Phys. Rev. D* **12**, 147 (1975).
- [67] Y. R. Liu, H. X. Chen, W. Chen, X. Liu, and S. L. Zhu, Pentaquark and tetraquark states, *Prog. Part. Nucl. Phys.* **107**, 237 (2019).
- [68] L. Zhao, W. Z. Deng, and S. L. Zhu, Hidden-charm tetraquarks and charged Z_c states, *Phys. Rev. D* **90**, 094031 (2014).
- [69] K. Chen, X. Liu, J. Wu, Y. R. Liu, and S. L. Zhu, Triply heavy tetraquark states with the $QQ\bar{Q}\bar{q}$ configuration, *Eur. Phys. J. A* **53**, 5 (2017).

- [70] S. Q. Luo, K. Chen, X. Liu, Y. R. Liu, and S. L. Zhu, Exotic tetraquark states with the $qq\bar{Q}\bar{Q}$ configuration, *Eur. Phys. J. C* **77**, 709 (2017).
- [71] J. Wu, Y. R. Liu, K. Chen, X. Liu, and S. L. Zhu, Heavy-flavored tetraquark states with the $QQ\bar{Q}\bar{Q}$ configuration, *Phys. Rev. D* **97**, 094015 (2018).
- [72] J. Wu, Y. R. Liu, K. Chen, X. Liu, and S. L. Zhu, $X(4140)$, $X(4270)$, $X(4500)$ and $X(4700)$ and their $c\bar{s}c\bar{s}$ tetraquark partners, *Phys. Rev. D* **94**, 094031 (2016).
- [73] J. Wu, X. Liu, Y. R. Liu, and S. L. Zhu, Systematic studies of charmonium-, bottomonium-, and B_c -like tetraquark states, *Phys. Rev. D* **99**, 014037 (2019).
- [74] J. Wu, Y. R. Liu, K. Chen, X. Liu, and S. L. Zhu, Hidden-charm pentaquarks and their hidden-bottom and B_c -like partner states, *Phys. Rev. D* **95**, 034002 (2017).
- [75] Q. S. Zhou, K. Chen, X. Liu, Y. R. Liu, and S. L. Zhu, Surveying exotic pentaquarks with the typical $QQq\bar{q}\bar{q}$ configuration, *Phys. Rev. C* **98**, 045204 (2018).
- [76] S. Y. Li, Y. R. Liu, Y. N. Liu, Z. G. Si, and J. Wu, Pentaquark states with the $QQQq\bar{q}$ configuration in a simple model, *Eur. Phys. J. C* **79**, 87 (2019).
- [77] H. T. An, Q. S. Zhou, Z. W. Liu, Y. R. Liu, and X. Liu, Exotic pentaquark states with the $qqQQ\bar{Q}$ configuration, *Phys. Rev. D* **100**, 056004 (2019).
- [78] Y. R. Liu, X. Liu, and S. L. Zhu, $X(5568)$ and its partner states, *Phys. Rev. D* **93**, 074023 (2016).
- [79] J. B. Cheng and Y. R. Liu, Understanding the structures of hidden-charm pentaquarks in a simple model, *Nucl. Part. Phys. Proc.* **309–311**, 158 (2020).
- [80] J. B. Cheng and Y. R. Liu, $P_c(4457)^+$, $P_c(4440)^+$, and $P_c(4312)^+$: Molecules or compact pentaquarks?, *Phys. Rev. D* **100**, 054002 (2019).
- [81] J. B. Cheng, S. Y. Li, Y. R. Liu, Y. N. Liu, Z. G. Si, and T. Yao, Spectrum and rearrangement decays of tetraquark states with four different flavors, *Phys. Rev. D* **101**, 114017 (2020).
- [82] H. T. An, K. Chen, Z. W. Liu, and X. Liu, Fully heavy pentaquarks, *Phys. Rev. D* **103**, 074006 (2021).
- [83] H. Hogaasen, E. Kou, J. M. Richard, and P. Sorba, Isovector and hidden-beauty partners of the $X(3872)$, *Phys. Lett. B* **732**, 97 (2014).
- [84] M. Karliner, S. Nussinov, and J. L. Rosner, $QQ\bar{Q}\bar{Q}$ states: Masses, production, and decays, *Phys. Rev. D* **95**, 034011 (2017).
- [85] X. Z. Weng, X. L. Chen, and W. Z. Deng, Masses of doubly heavy-quark baryons in an extended chromomagnetic model, *Phys. Rev. D* **97**, 054008 (2018).
- [86] X. Z. Weng, X. L. Chen, W. Z. Deng, and S. L. Zhu, Hidden-charm pentaquarks and P_c states, *Phys. Rev. D* **100**, 016014 (2019).
- [87] X. Z. Weng, X. L. Chen, W. Z. Deng, and S. L. Zhu, Systematics of fully heavy tetraquarks, *Phys. Rev. D* **103**, 034001 (2021).
- [88] X. Z. Weng, W. Z. Deng, and S. L. Zhu, Doubly heavy tetraquarks in an extended chromomagnetic model, *Chin. Phys. C* **46**, 013102 (2022).
- [89] S. Godfrey and N. Isgur, Mesons in a relativized quark model with chromodynamics, *Phys. Rev. D* **32**, 189 (1985).